TNO innovation for life

Report of RealCOE WP 7.6: Evaluation of Different Grid Connection Concepts

TNO Internal ⟩ TNO 2024 Rxxxxx
24 January 2025

Energy & Materials Transition
www.tno.nl
+31 88 866 50 65
info@tno.nl

TNO 2024 Rxxxxx – 24 January 2025

Report of RealCOE WP 7.6: Evaluation of Different Grid Connection Concepts

Author(s) Mojtaba Moradi-Sepahvand
Classification report TNO Internal
Number of pages 77 (excl. front and back cover)

Summary

This project introduces a comprehensive framework to enhance the efficiency and reliability of offshore wind farm (OWF) collection grid design. By addressing critical aspects of OWF planning and operation, it evaluates emerging trends and technological advancements to identify economically viable connection configurations while exploring pathways to accommodate larger and more efficient wind farms. Special emphasis is placed on the role of high-voltage AC and VSC-based DC transmission systems in optimizing both design and operational performance.

Central to this research is the development of an advanced optimization model for offshore wind farm cable routing and offshore substation siting and sizing, utilizing a Mixed-Integer Linear Programming (MILP) approach. The model aims to minimize total costs, encompassing both capital and operational expenses (including cable and VSC losses, as well as wind energy curtailment), while maximizing revenue. Key input parameters include historical wind speed and direction data, turbine power curves, cable specifications, and hourly energy market prices. The optimization framework incorporates sophisticated techniques such as interpolation to dynamically estimate power output, the lower convex envelope linearization methodology to accurately calculate energy losses in medium-voltage inter-array and high-voltage transmission cables as well as VSCs, and grid-based layouts to maximize energy capture while mitigating wake effects.

The findings validate the efficacy of the proposed MILP optimization framework through comprehensive scenario analysis, demonstrating its effectiveness in addressing key challenges in offshore wind farm collection grid design. The study evaluates various configurations, including radial, ring, and star layouts, highlighting their distinct advantages and trade-offs, particularly in the context of reliability under medium-voltage (MV) cable contingencies. The star configuration, despite higher initial investment costs due to its dedicated cable connections from each turbine to the offshore substation, emerges as a robust solution. This design effectively isolates the impact of a cable failure to a single turbine, ensuring uninterrupted operation for the rest of the system. Its fault isolation capability enhances both reliability and profitability, making it particularly suitable for scenarios with frequent cable contingencies or where high operational uptime is critical. The ring configuration offers a balanced approach by incorporating redundancy into the collection grid. Each turbine is connected to the offshore substation through two independent pathways, which ensure an alternative route for power transfer during a single cable failure. This redundancy enhances fault tolerance and minimizes the risk of widespread energy curtailment. Although the ring configuration entails slightly higher investment costs compared to radial configurations, its capacity to sustain power flow during cable outages guarantees stable and efficient grid operation. In contrast, the radial configuration, known for its simplicity and cost-effectiveness, stands out as the most economical option under normal operating conditions. However, it is highly vulnerable to cascading failures in the event of a cable outage. A single cable failure can disrupt power transfer for an entire branch of turbines, resulting in significant energy curtailment and economic losses. This limitation highlights the importance of adopting more resilient designs, such as the star or ring configurations, in scenarios where system reliability and fault tolerance are critical. These comparative insights emphasize the need to align grid configuration choices with specific operational requirements and contingency planning priorities. The MILP framework facilitates a detailed evaluation of these trade-offs, which enables decision-makers to select the most suitable design based on project-specific objectives, such as minimizing costs, maximizing reliability, or achieving a bal-

anced approach. The ability to model and optimize diverse scenarios highlights the robustness of the proposed framework in guiding the development of efficient and reliable offshore wind farm collection grids.

The research highlights the critical role of optimizing offshore substation placement in enhancing the overall performance and economic viability of OWFs. By comparing fixed substation locations with scenarios featuring multiple candidate locations, the study demonstrates financial advantages achieved through strategic substation placement. Optimal siting minimizes cable losses and operational costs, leading to an increase in revenue. This finding shows the transformative potential of integrating substation optimal placement into the planning and design phases of OWFs.

Ultimately, this project contributes to the advancement of offshore wind energy by offering practical strategies and detailed insights for designing cost-effective, reliable, and efficient collection grids. By supporting the transition to renewable energy, this research contributes to global efforts to achieve decarbonization and energy security, essential for building a greener and more sustainable future.

The source code for this project, i.e., **OWFOptimizer**, is publicly available is available on GitLab at `https://gitlab.tsn.tno.nl/moradisepahvandm/OWFOptimizer`.

Contents

List of Figures

List of Tables

1 Introduction

The ongoing global transition toward renewable energy sources has placed offshore wind farms (OWFs) at the forefront of sustainable electricity generation. OWFs leverage the abundant and consistent wind resources over the oceans to produce clean energy, offering a reliable alternative to traditional fossil fuel-based systems. By harnessing higher wind speeds and steadier wind patterns compared to onshore installations, offshore OWFs have become a critical component in achieving net-zero emission goals. However, their development also introduces significant engineering and economic challenges, particularly in the design and optimization of collection grid systems.

Within the Real COE project's Work Package (WP) 7.6, the primary focus is to develop an efficient grid connection concept tailored for offshore wind farms. The collection grid serves as the backbone of the OWF electrical system, consolidating the electricity generated by numerous turbines dispersed over extensive maritime areas. This energy is transferred to a centralized offshore substation, where it is stepped up in voltage for efficient long-distance transmission to onshore power grids via high-voltage undersea cables. The design and performance of the collection grid system directly impact the efficiency, reliability, and cost-effectiveness of offshore wind energy production.

The offshore environment presents unique challenges for OWF collection grid systems. Harsh marine conditions necessitate robust engineering solutions to ensure the durability of critical infrastructure, including inter-array and export cables, as well as substations. Furthermore, the variable and often unpredictable nature of wind speeds adds complexity to grid design, requiring advanced optimization techniques to balance energy capture, transmission efficiency, and overall costs. Addressing these challenges is essential for scaling up offshore wind installations to meet future energy demands.

This report outlines the project's objectives and contributions, with a primary aim of enhancing the efficiency and reliability of OWF collection grids. The project investigates key challenges, such as optimizing grid configurations for variable wind conditions, selecting optimal offshore substation locations, and incorporating high-voltage AC and DC transmission solutions to improve operational performance. By leveraging advanced modeling and optimization methodologies, the project seeks to provide actionable insights for addressing these challenges and driving innovation in offshore wind energy systems.

The report is structured to guide the reader through the critical aspects of the project. It begins with an overview of the project's scope and goals, followed by a comprehensive literature review to situate the research within the current state of the art. Subsequent sections detail the problem formulation and modeling approaches, which integrate mixed-integer linear programming (MILP) to optimize cable routing, substation placement, and overall system configuration. The results of the analysis are presented and discussed, providing insights into the comparative performance of different grid configurations, including radial, ring, and star layouts. Finally, the findings are synthesized into actionable recommendations for advancing OWF design, with considerations for economic and operational factors.

This work aims not only to address immediate challenges in OWF grid design but also to set the stage for future advancements in sustainable energy systems. By delivering cost-effective and reliable solutions, the outcomes of this project contribute to the broader goal of transitioning

to a decarbonized energy landscape.

2 Problem Definition and Main Goals

This project aims to establish a comprehensive framework to enhance the efficiency, reliability, and cost-effectiveness of offshore wind farm (OWF) collection grids. By systematically addressing critical design and operational challenges, this research explores innovative solutions that can support the sustainable growth of offshore wind energy systems. The project focuses on three interrelated objectives:

2.1 Objective 1: Optimizing Offshore Wind Farm Collection Grid Configurations

This objective provides a foundation for designing OWF collection grids by analyzing current practices and exploring innovative opportunities:

- **Trend Analysis:** A detailed evaluation of existing grid configurations, industry advancements, and emerging technologies to identify best practices and performance gaps. This analysis highlights potential avenues for improvement in grid design and operation.
- **Upscaling Potential:** Investigating strategies to accommodate larger wind farms with increased turbine capacities. This includes optimizing spatial configurations, interconnection strategies, and exploring advanced materials to improve performance and reduce costs.
- **Cost Assessment:** Conducting a thorough cost-benefit analysis of different grid configurations to balance investment, operational expenses, and revenue optimization. The findings guide the adoption of economically viable and technically efficient configurations.

The outcomes aim to equip offshore wind farms with scalable and future-ready collection grid frameworks.

2.2 Objective 2: Enhancing Offshore Substation Placement and Transmission Systems

This objective addresses the critical role of offshore substations and transmission technologies in OWF performance:

- **Substation Optimization:** Developing optimization methodologies to strategically locate offshore substations, minimizing cable losses, reducing costs, and maximizing energy delivery efficiency.
- **Transmission System Evaluation:** Assessing the feasibility and performance of high-voltage AC (HVAC) and voltage source converter-based HVDC (VSC-HVDC) systems for connecting offshore substations to onshore power grids.

- **Operational Impacts:** Analyzing the reliability, efficiency, and long-term operational costs of various transmission systems under diverse scenarios, including those involving remote offshore wind farms.

This objective ensures that design choices for transmission systems and substations enhance the technical and financial viability of OWFs.

2.3 Objective 3: Reliability and Flexibility of OWF Systems

This objective focuses on designing resilient and adaptive OWF systems to meet future energy demands:

- **Reliability Analysis:** Investigating the resilience of radial, ring, and star collection grid configurations under fault scenarios, such as cable outages. This ensures minimal energy curtailment and maximum fault tolerance.
- **Dynamic Adaptability:** Enhancing offshore wind farms' ability to adapt to changing wind conditions and grid demands by analyzing representative data of wind turbine output power and electricity market. This approach ensures optimized operations, improved grid balance, and maximized energy capture.
- **Efficient Grid Integration:** Facilitating the efficient integration of offshore wind farms into power grids by evaluating hybrid HVAC/HVDC transmission systems, assessing advanced grid support features, and ensuring compatibility with existing infrastructure to enhance grid stability, reliability, and efficiency.

This objective emphasizes the need for robust and flexible offshore wind farm designs that contribute to the long-term stability and adaptability of the power grid.

3 Literature Survey

The integration of OWF into the global energy mix is an essential step towards achieving a sustainable and carbon-neutral future. OWFs, benefiting from the sea's constant and strong winds, offer a reliable and substantial source of RES. This shift is imperative in today's rapidly changing energy landscape, where the emphasis is increasingly on RESs such as wind and solar power to mitigate climate change impacts.

As the world moves away from fossil fuel dependency, the challenge of integrating remote RESs with existing power grids becomes apparent. The distance between OWFs and consumer centers presents technical, financial, and logistical challenges which necessitate advancements in grid capacity and stability. Ensuring the continuous and reliable operation of this critical infrastructure, alongside addressing cybersecurity risks brought about by digitalization, is very important.

The role of RESs, including both onshore and OWFs, is becoming more significant, contributing to a considerable reduction in carbon dioxide emissions. Specifically, OWF requires robust grid connections to transport electricity from production sites in the North sea to land-based consumers. This process involves complex coordination between OWF design and grid connection planning to synchronize work and minimize financial risks.

Transmission technologies are evolving to address the challenges of connecting OWFs to onshore grids efficiently. Current proposals include high voltage alternating current (HVAC), high voltage direct current (HVDC), and low-frequency alternating current (LFAC) or fractional frequency AC transmission, each with its advantages and considerations depending on distance and technical requirements [1]. Specifically, LFAC transmission is notable for its efficiency in extending transmission distances and capacities by operating at a reduced system frequency, which optimizes charging power, reduces skin effects, and enhances real power capacity [2, 3].

The installation and operational complexities of OWFs are greater compared to their onshore counterparts. These complexities necessitate innovative approaches in construction, installation, and power transmission. The literature suggests a preference for HVDC transmission systems for long-distance integration of OWFs to overcome limitations related to AC cables such as cable charging current and reactive power loss [4], [5]. Recent studies also explore hybrid-HVDC and diode rectifier-based HVDC (DR-HVDC) systems based on LCC and VSC technologies, aiming to reduce costs and improve efficiency in OWF integration [6], [7], [8]. DR-HVDC systems represent an innovative approach in the field of electrical engineering, particularly in the transmission of power from RESs like OWFs to the main grid. Unlike traditional HVDC systems, which typically use complex and expensive converter technology for converting AC to DC and vice versa, DR-HVDC systems simplify the rectification process by employing diodes. By employing diodes, which are generally cheaper than active converter components like thyristors and insulated gate bipolar transistors (IGBTs), DR-HVDC systems reduce the overall cost of the transmission infrastructure. While DR-HVDC offers several advantages, it also faces limitations, particularly in terms of control and flexibility. Unlike active converter-based systems (e.g., VSC-HVDC), DR-HVDC systems offer limited control over the power flow, making them less adaptable to rapidly changing grid conditions. Additionally, the lack of reversal capability in current flow means that DR-HVDC systems are primarily suited for unidirectional power transmission. A study on the control of parallel operation of DR-HVDC and VSC-HVDC links connected to OWFs

is presented in [7]. That study focused on a grid-forming control strategy, where VSC-HVDC manages voltage and frequency for OWF startup, and DR-HVDC handles power transmission once operational. This approach allows for the VSC-HVDC to be sized for system energization, with the bulk of power transmission handled by the more cost-effective DR-HVDC. Continued innovation and development in this field are likely to further enhance the viability and efficiency of DR-HVDC systems which can make them an integral part of the world RES infrastructure.

Globally, Europe leads in the installed capacity of OWF, followed by Asia and America, reflecting the significant potential and growing reliance on this RESs [3]. The development and deployment of advanced power transmission technologies are crucial in harnessing OWF's full potential, ensuring its efficient integration into the global energy system, and paving the way towards a more sustainable and climate-resilient future.

3.1 Offshore Wind AC Collection Grid Topology

Offshore wind farms with turbine capacities in the megawatt (MW) range, collectively contribute to significant power generation. These farms which are capable of producing from a few hundred to several thousand MW, require robust interconnections with the mainland power grid. This necessitates the collection grid, a critical infrastructure designed to link all wind turbine generators (WTG) for efficient energy transmission over long distances. The configuration of an offshore wind farm's collection grid is crucial, as it influences the length of undersea cables and the setup of electrical parameters and connections.

AC collection grids have become the standardized approach in constructing offshore wind farms. This section aims to elucidate the concept of AC collection grids for offshore wind power applications. The primary topologies identified include radial, ring, and star configurations, which have emerged as leading models for these grids [9, 10, 11]. Moreover, a range of hybrid or composite topologies has been introduced, which indicate the potential for innovative design approaches [12]. While other topologies are present, they are generally seen as variations of these primary models. Therefore, an analysis of these fundamental topologies provides a thorough understanding of AC collection grids. The critical components of AC collection grids are cables, connectors, and transformers.

Choosing an appropriate topology is influenced by various factors, such as the capacity of the wind farm, its distance to the mainland grid, and the system's reliability standards. This choice is critical, as it affects undersea cable lengths, electrical parameters, and the configurations of electronic devices linking the farm to the grid. Therefore, these factors play a decisive role in determining the reliability and efficiency of the offshore wind farm's connection to the onshore grid. An examination of the three primary collection grid topology configurations is presented in the following sections.

- **Radial:** Radial clusters enable wind turbines to integrate their power into a unified feeder in which wind turbines are configured in series. In this regard the feeder bus is adjusted to a high enough voltage to accommodate the sum of power produced by the feeder. To Address the variance in voltage between WTGs and the feeder bus, each turbine requires the installation of a step-up transformer to increase the output voltage. The radial configuration, as shown in Figure 3.1, is distinguished by its operational simplicity and economic viability, although it is compromised by reliability concerns. Any instance necessitating maintenance of the network cable or its associated equipment, forces the disconnection of the entire system. Nevertheless, the radial collection framework remains the most economically favorable and very commonly adopted grid topology in

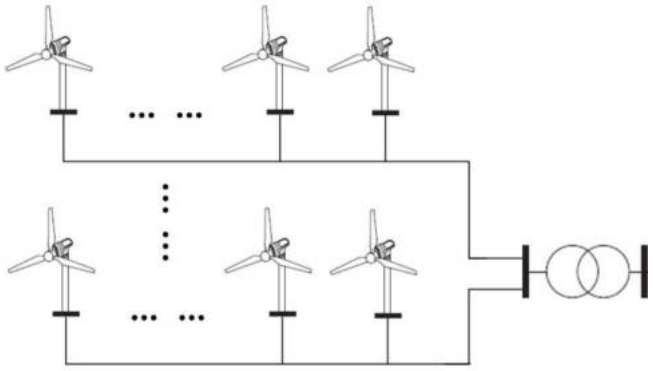

Figure 3.1: Radial Connection Configuration for Collecting Offshore Wind Farms Generated Power

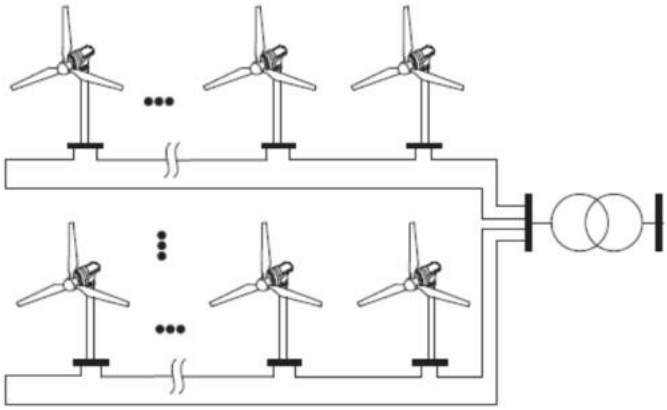

Figure 3.2: Ring Connection Configuration for Collecting Offshore Wind Farms Generated Power

current use. This approach has been extensively applied across numerous offshore wind projects, with Denmark's Horns Rev2 wind farm serving as a prime example [13].

- **Ring:** In offshore wind farms, the ring connection configuration links wind turbines in a circular pattern which create a closed loop. This design, as shown in Figure 3.2, significantly increase the system's resilience by providing an alternate circuit for electricity in the event of a failure in any line or component. It simplifies maintenance operations and minimizes the likelihood of total power failures. Nonetheless, the increased reliability and flexibility come with higher complexity and cost, marking a trade-off against more straightforward configurations such as the radial connection.

- **Star:** Within the star collection system, as shown in Figure 3.3, each WTG establishes a direct connection to a nodal point via cables, which vary in capacity from small to medium, and incorporates a transformer situated on the offshore platform. Subsequent to this transformer, the cumulatively generated electricity is transferred to a central collection point through cables of larger capacity. The star topology is renowned for its exceptional reliability; however, it introduces certain limitations. The requirement for a greater assortment of electrical equipment, such as circuit breakers and isolating switches, renders this topology financially less attractive compared to other topologies. As a result, its implementation within wind farms is typically reserved for situations characterized by distinct demands.

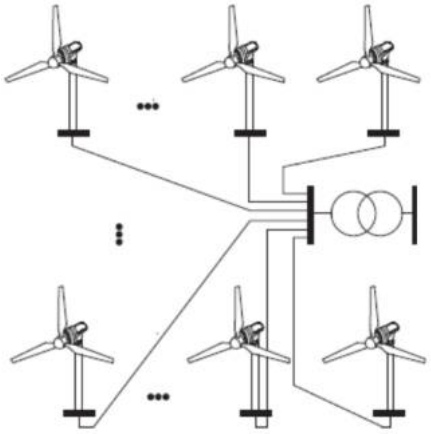

Figure 3.3: Star Connection Configuration for Collecting Offshore Wind Farms Generated Power

3.1.1 AC Collection Voltage Level

Typically, the voltage levels for offshore AC collection grids fall within the medium-voltage range to facilitate the efficient collection and initial transmission of power before it is stepped up to a higher voltage for long-distance transmission. Currently, there is no commercial standard established for voltage level of AC collection grid in offshore wind farms [9]. However, the AC collection grids voltage level typically spans from 11 kV up to 36 kV. Most of the designs are in 11 kV range. Some newer and larger projects might utilize voltages towards the higher end of this range (33 and 36 kV) to reduce losses and improve efficiency [14].

3.1.2 Cost of AC Collection Grids

The cost of AC collection grids for offshore wind farms varies depending on the topology used. For instance, ring formation systems can have a capital cost 2.5 to 5 times higher than star or radial topologies for a collector system of 33 kV [9]. However, smaller offshore wind farms below 100 MW often opt for less redundancy to reduce installation costs. The choice of topology significantly impacts the overall investment and operational expenses.

3.1.3 AC Cables

In offshore wind farms, there are two main types of cables: *inter-array* and *export cables*. Inter-array cables connect individual turbines to each other and to the offshore substation, typically operating within a voltage range of 33 to 66 kV. Export cables transfer power from the offshore substation to the onshore grid connection point at voltages of 132 kV or higher, designed to handle larger amounts of power over longer distances with reduced losses. The most common type of subsea AC cable used in offshore wind farms features cross-linked polyethylene (XLPE) insulation with a copper conductor. XLPE cables are used both as inter-array cables, typically rated between 33 kV and 66 kV, and as export cables, which can be rated up to 220 kV or higher. In addition to XLPE cables, Ethylene Propylene Rubber (EPR) cables can also be used for inter-array connections. These cables, less commonly used than XLPE, are more flexible and can be advantageous during installation and in dynamic cable applications where movement is expected.

Generally, depending on the physical stresses of cable installation locations, they can be categorized into static and dynamic cables. Static power cables in offshore wind farms are used for connections that do not require frequent movement. They are typically installed on the

seabed between turbines in a wind farm (inter-array cables) and from the wind farm to the shore (export cables). On the other hand, dynamic power cables are essential for applications where the cable needs to withstand mechanical loads and movements. These are commonly used in floating wind turbines, which are anchored to the seabed but can move with the wind and waves. A dynamic cable is estimated to be 30–60% more expensive than a static cable for a system voltage of around 36 kV [9].

3.1.4 Transformers

Transformers play a crucial role in power systems and are used for a variety of functions. They come in numerous forms, each customized for particular needs. These devices can operate in either dry or wet conditions and use various types of insulation based on the safety needs of the environment. Commonly, transformers are either oil-filled, referred to as liquid-immersed, or air-insulated, known as dry-type transformers. On land, AC transformers designed to handle more than 1000 MVA and 800 kV are commonly employed. The selection of insulation material is vital for offshore applications due to the potential environmental consequences of their failure. Although transformers suited for moist conditions are available on the market, they have not achieved the same levels of power and voltage as their dry-environment counterparts. Various manufacturers provide options up to 145 kV and 100 MVA [15, 16]. Structurally, a wet-environment transformer mirrors a dry-environment one but includes a liquid filling and is pressurized to align with the subsea depth pressures. The cost of a dry-type transformer is about 1.3 times that of a comparable liquid-immersed transformer, while a transformer designed for wet environments may cost up to seven times more than one intended for dry conditions.

3.2 Offshore Wind DC Collection Grid Topology

This section introduces the various topologies applicable for DC collection grids in offshore wind farm setups. Currently, AC collection systems serve as the prevalent model for the construction of offshore wind farms due to the ready availability of protective technologies and their well-established framework. Nevertheless, the potential of DC collection grids has begun to capture attention, with advancements in protective solutions making them a viable option. While large-scale operational examples of DC wind farms are yet to be realized, the pursuit of research and the development of small-scale models indicate a growing interest in this technology globally [9]. Moreover, the transmission of power from offshore wind farms, particularly those located at significant distances from the coast, commonly employs HVDC systems. However, the internal networks within these farms typically continue to rely on AC solutions [14]. An illustrative representation of the overall composition of an offshore wind farm is provided in Figure 3.4 [17].

The implementation of DC collection grids within offshore wind farms involves the amplification of generator voltage to a medium level through the use of power converters. These systems employ medium-voltage submarine DC cables for the linkage of wind-energy conversion systems to a central DC platform. The exploration and consideration of DC grid systems are driven by the prospect of reduced capital costs and enhanced reliability for large offshore wind farms, particularly those positioned further from coastal lines to leverage more substantial wind resources [17]. Generally, as shown in Figure 3.5, there are three DC collection grid topologies, including parallel, series, and series-parallel. The connection system between each of the turbine generators and DC converters in a DC collection grid topology is illustrated in Figure 3.6 [10].

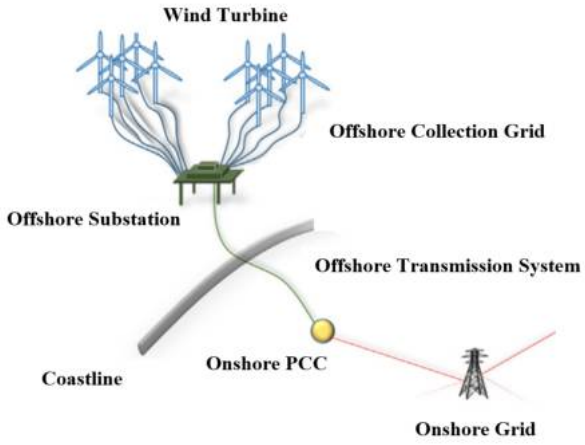

Figure 3.4: Schematic Overview of an Offshore Wind Farm

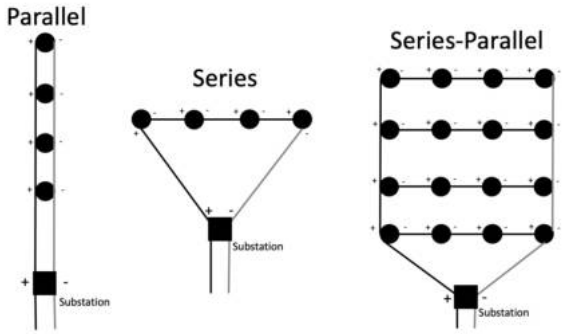

Figure 3.5: DC Collection Grid Topologies for Offshore Wind Farms

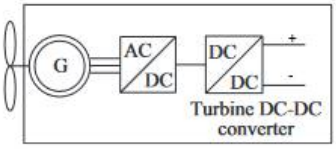

Figure 3.6: Turbine generators connection in a DC Collection Grid Topology

- **Parallel Configuration**: In a parallel configuration, as depicted in Figure 3.7, all components (such as wind turbines) are connected such that the voltage across each one is the same and the total current is the sum of the currents through each component. This setup maintains a consistent voltage level across the array and allows for flexibility in adding or removing components without significantly impacting the overall system voltage. A parallel configuration is common in applications where maintaining a stable voltage is important and where individual components might need to be isolated or disconnected without affecting the entire system.

- **Series Configuration**: In a series configuration, as illustrated in Figure 3.8, components are connected end-to-end, so the current flowing through each component is the same, and the total voltage is the sum of the voltages across each component. A series configuration is useful for increasing the voltage level of the entire system without requiring high-voltage components. This configuration is used in systems where space is limited or where high voltage is required, but each component produces a relatively low voltage.

- **Series-Parallel Configuration**: This configuration combines elements of both series and parallel setups. Some components are connected in series to increase the voltage, while these series groups are then connected in parallel to increase the current capacity. The series-parallel configuration allows for optimization of both voltage and current within the system, providing a balance that can be tailored to specific power requirements and operational conditions. This configuration is typically used in larger installations where both high voltage and high current are necessary, such as in sections of wind farms where multiple turbines need to be efficiently integrated into the power grid. Moreover, series-parallel configuration can save the offshore HVDC stations.

  In [18] the utilization of DC series-parallel collection systems for integrating offshore wind farms is explored. This paper tries to deal with the wind power curtailment challenge inherent in offshore wind farms. Through mathematical analysis, it devises an optimization model that accounts for wind power curtailment. Evaluation on a 56-turbine offshore wind farm demonstrates the benefits of considering wind power curtailment during planning which can lead to cost savings in the long horizon. Furthermore, it suggests optimizing the layout of the series wiring to align with prevailing wind directions to enhance power generation efficiency and lowering expenses.

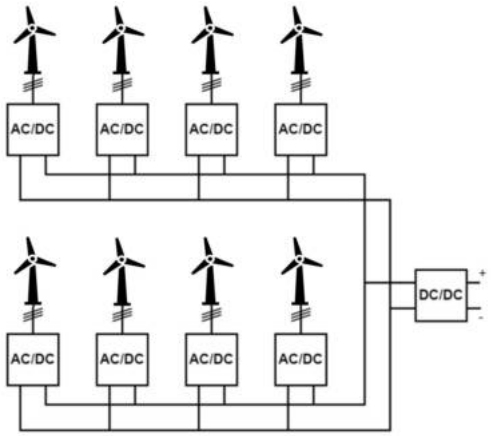

Figure 3.7: Parallel Configuration in a DC Collection Grid

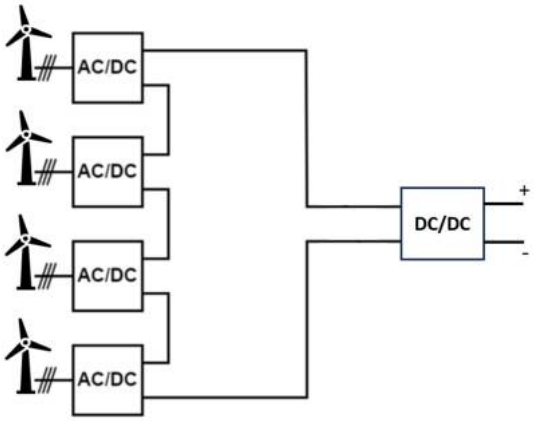

Figure 3.8: Series Configuration in a DC Collection Grid

The study in [19] introduces a concept called the multifunctional DC collector (MDC) for constructing efficient and cost-effective all-DC offshore wind power systems. The MDC serves to smooth energy collection and boost processes to reduce system costs and complexities while enhancing reliability and flexibility. By implementing MDC, inter-turbine coupling is minimized which can enable each wind turbine unit to operate independently. The challenges associated with series networking approaches and the limitations of existing solutions are highlighted in [19]. In general, the proposed MDC can be a practical pathway for the development of large-scale offshore wind farms.

- **Choosing Between AC and DC Collection Grids for Wind Farms:** Offshore wind farms that utilize HVDC transmission have the option to implement either an AC or DC collection grid. The conversion from a medium voltage AC grid to an HVDC transmission system requires the use of complex equipment, such as large transformers and power electronics converters. This complexity leads to the construction of extensive offshore platforms and increases the maintenance demands for the transformers due to power frequency adjustments. Opting for a medium voltage DC collection grid is seen as a progressive approach which can mitigate these issues through recent technological innovations.

  A medium voltage DC collection grid is strategically advantageous compared to its AC alternative, primarily because it bypasses issues related to reactive power and potential resonance effects. It ensures a consistent output voltage from each wind turbine without necessitating an initial voltage step-up, thereby reducing switching losses. While a DC system still requires a booster station, the space needed for a DC booster's power electronics converter is significantly smaller. This approach offers additional benefits, such as cost savings on generator drives and enhanced overall system reliability, by eliminating the need for a Voltage Source Converter (VSC) at each turbine location.

  In [20] Offshore Wind farm Layout (OWL) optimizer tool is developed for optimizing offshore wind farm electrical layouts, achieving cost savings and efficiency improvements. By using techniques like MIP and Benders' decomposition, the model in In [20] tried to reduce computation time and accounts for key variables like wind variability and component failures. An integer linear programming models to optimize the cable network in wind farms is proposed in [21]. The main goal of the model in [21] was minimizing both infrastructure costs and energy loss costs while considering technical constraints. In [22] a two-layer hybrid optimization approach for planning of large-scale offshore wind farms is proposed with aiming to balance economic efficiency and output stability in the collector system. The method in [22] combines deterministic and heuristic algorithms to optimize the placement and clustering of wind turbines and substations, as well as the cable connections within each cluster. The outer layer of the hybrid model utilizes fuzzy C-means clustering and genetic algorithms to partition wind turbines into groups and determine optimal substation locations for effective power collection and transmission. The inner layer employs genetic algorithms integrated with the deterministic Clark and Wright's saving algorithm to arrange optimal cabling within these groups, aiming to minimize both initial investment costs and long-term power loss.

  In [23] an approach to assessing the reliability of large-scale offshore wind farms is introduced by integrating multi-state Markov processes with the universal generating function. The approach simplifies computational efforts by dividing the network into feeders while maintaining dependencies between wind turbine outputs. The study in [23] highlights the importance of considering inter-array cable reliability due to significant repair times and their impact on farm output. The study also suggests replacing traditional binary reliability models with multi-state models to capture the complex failure dynamics of wind farm components more accurately.

In [24], a multi-layer optimization framework is proposed that combines cross-substation incorporation (CSI) with radial topology to enhance power-sharing capabilities among substations. The framework's three layers—offshore substation refinement, offshore wind farm partition, and intra-zone cable connection—jointly optimize the collector system, which can address the unique challenges presented by wind turbine capacity deviations and the need for efficient cable routing. Moreover, the authors of [24] enhance existing algorithms, such as the minimum spanning tree and Clark and Wright's saving algorithms, to account for cable type selection and the avoidance of cable crossings. Their approach is validated through comparative studies with traditional radial and ring topologies.

3.3 Overview of Offshore Energy Transmission Systems

To minimize transmission losses and current ratings of equipment, large offshore energy farms use either HVAC or HVDC systems to transport electricity power to shore. Initially, large offshore wind farms employed HVAC for this purpose. Yet, with the growth in farm size and the extension of distances to shore, the adoption of HVDC technology has risen [25]. The main reason for using HVAC is the possibility of utilizing standard transformers to change the voltage levels and the simple design of protection systems compared with HVDC.

An overhead HVAC transmission line can typically be categorized in three types depending on the length, short, medium, and long lines [26].

- **Short lines:** Short lines are typically less than 80 kilometers in length. At these distances, the capacitive effects of the line are usually negligible, so they are often ignored in calculations. The primary concerns with short lines are the resistance and inductance of the conductors, which cause voltage drops and power losses.

- **Medium lines:** Ranging between 80 kilometers and 250 kilometers, medium lines exhibit significant capacitive properties. For these lines, the capacitance starts to have a noticeable effect on the performance of the transmission line. The modeling of these lines is more complex and often involves considering the line as a series of distributed inductance, resistance, and capacitance (distributed parameters).

- **Long lines:** These are lines that extend beyond 250 kilometers. Long lines require a more detailed model that includes all the distributed parameters. The effects of the line's capacitance become even more noticeable, impacting not just the voltage along the line due to reactive power flow but also the stability and control of power transmission. These lines are often modeled using hyperbolic functions or by using numerical methods to solve the transmission line equations.

Submarine HVAC cables are characterized by high capacitance, leading to resonance complications and a decrease in power transmission capacity due to the raised charging currents. Long cables with significant charging currents may require the use of Static VAR compensators for mitigation. This solution, however, is technically demanding and financially expensive. Ideally, compensation should be distributed at multiple points along the cable, but practical constraints usually confine installation to just the ends of the cable. In contrast, HVDC cables experience little or no charging current, which not only reduces losses and voltage drop but also

increases the transferable power capacity relative to HVAC systems, thereby obviating the need for expensive compensation units. Additionally, HVAC systems connected synchronously to the grid are prone to fault propagation, which means a fault in one part of the grid can affect other areas. However, HVDC grids, due to their lack of synchronous connection, do not substantially affect the short-circuit current in the main HVAC grid. Another advantage of HVDC, especially when combined with voltage source converter (VSC) technology, is the capability to provide ancillary services to the main HVAC grid. This includes quick adjustments to active and reactive power and frequency response, enhancing grid stability and functionality. Expanding on these topics, the review in [27] discusses the role of dynamic modeling in HVDC systems, emphasizing their efficiency in managing reactive power and improving system stability, which is crucial for long-distance, high-capacity power transmissions. They also highlight how HVDC, particularly through VSCs, enhances grid stability by enabling rapid control mechanisms that adapt to fluctuations, thus supporting grid services more effectively than traditional HVAC systems. These findings confirm the operational advantages of HVDC in modern power systems.

One limitation of HVDC transmission is that it requires more power electronic components than traditional HVAC systems, which raises initial investment costs. The construction of AC/DC and DC/AC converter stations also contributes significantly to these higher costs. However, HVDC tends to have lower operational costs per kilometer due to reduced cable material needs and lesser power losses. Although HVDC has higher upfront costs, it becomes more cost-effective than HVAC at greater distances. Several studies have evaluated the break-even distance—the point where the costs of HVDC and HVAC equalize. For example, research suggests that for lower capacity systems (like a 100 MW wind farm), this distance might be around 90 km, while for larger systems (like a 1 GW farm), it extends to 120-160 km. These distances vary based on factors including the need for reactive compensation, voltage levels, and rights-of-way.

4 Problem Modeling

In this section, we present a detailed formulation for modeling the offshore wind farm cable routing and offshore substation sitting and sizing problem as a Mixed-Integer Linear Programming (MILP) optimization. The optimization process involves a systematic approach that includes data collection, analytical techniques, and the use of specialized tools. The methodology adopted for this project is described below.

4.1 Introduction

The comprehensive formulations presented in this project for optimizing the collection grid of an offshore wind farm consist of several parts. The primary objective is to minimize the total cost, which includes both investment and operational expenses, and to maximize the total revenue. This must be achieved while ensuring technical feasibility and avoiding cable crossings. The following sections delve into the specifics of the MILP model, including the variables, constraints, and the overall optimization process. The approach consists of several key steps:

4.1.1 Data Collection

Comprehensive data is crucial for effective optimization. The data required includes:

- **Wind Speed and Direction Data:** Obtained from historical weather records specific to the offshore site. This data is used in conjunction with turbine power curves to calculate the wind factor for each hour of operation. Alternatively, if historical data of wind farm output power is available, the wind factor can be calculated directly without the need for turbine power curves.
- **Power Curve Data:** Provided by the turbine manufacturer, detailing the power output as a function of wind speed and direction. This curve is essential for estimating potential power generation, particularly when calculating the wind factor using wind speed and direction data.
- **Cables, HVAC, and HVDC System Specifications:** Includes costs, resistances, and capacities of different types of HVAC cables, HVDC cables, HVAC substation (including transformers), and HVDC converters. This information is critical for calculating both the investment and operational costs associated with the electrical infrastructure.
- **Energy Prices:** Hourly energy prices are used to calculate revenue from the generated power. This economic data is vital for determining the operational profitability of the offshore wind farm.

4.1.2 Analysis Techniques

Several analytical techniques are employed to solve the proposed complex optimization problem:

- **Interpolation:** To calculate the power output of turbines for varying wind speeds and directions, interpolation methods are applied over the given power curve data (see [28] for details on interpolation techniques).
- **Linear Programming:** The nonlinearity in the calculation of losses for both medium-voltage (MV) cables in the collection grid structure and high-voltage (HV) cables in the transmission side is linearized. Therefore, linear programming is utilized to formulate and solve the optimization problem.
- **Grid-Based Layout:** The turbines are arranged in a grid pattern to ensure uniform spacing which can optimize wind capture and minimize wake effects. This layout simplifies the design and enhances the efficiency of the wind farm.

4.1.3 Wind Farm Layout

The considered offshore wind farm consists of turbines arranged in a grid layout. The layout details are as follows:

- **Number of turbines:** 20
- **Arrangement:** 4 rows and 5 columns
- **Distance between turbines (columns):** 1500 meters
- **Distance between rows:** 1500 meters

The offshore substation candidate locations and the Point of Common Coupling (PCC) location are as follows:

- **Offshore Substation Location:** It is a *decision variable* in the model that can be optimized. In the initial phase of the simulation, for simplicity, a single fixed location is calculated based on the average position of the turbines. The position of fixed substations is calculated based on the following considerations:

  The fixed substation is positioned centrally relative to the turbine array. This central position is calculated as:

  $$\textbf{Fixed Substation X} = \frac{(\text{num of columns} - 1) \times \text{distance between turbines (columns)}}{2}$$

  $$\textbf{Fixed Substation Y} = -(\text{distance between rows})$$

  This ensures that the fixed substation is centrally located among the turbines, minimizing the average cable length required for connecting the turbines to the substation.

  In general, in addition to the mentioned fixed substation candidate location, the best candidate locations for offshore substations are obtained using a *hierarchical clustering*, as detailed in [29], to group the turbines based on their coordinates. The central locations within these clusters can then serve as potential candidate locations for the offshore substations.
- **PCC Location:** The fixed point onshore. PCC is centered between the columns and maintains a consistent distance offshore. The installed offshore substation can connect to the PCC via transformers and long HVAC cables or using a Voltage Source Converter (VSC) with HVDC cables. The distance between the PCC and the first row of turbines ranges from 60,000 to 100,000 meters, enabling the evaluation of the hybrid HVAC/HVDC transmission system's performance.

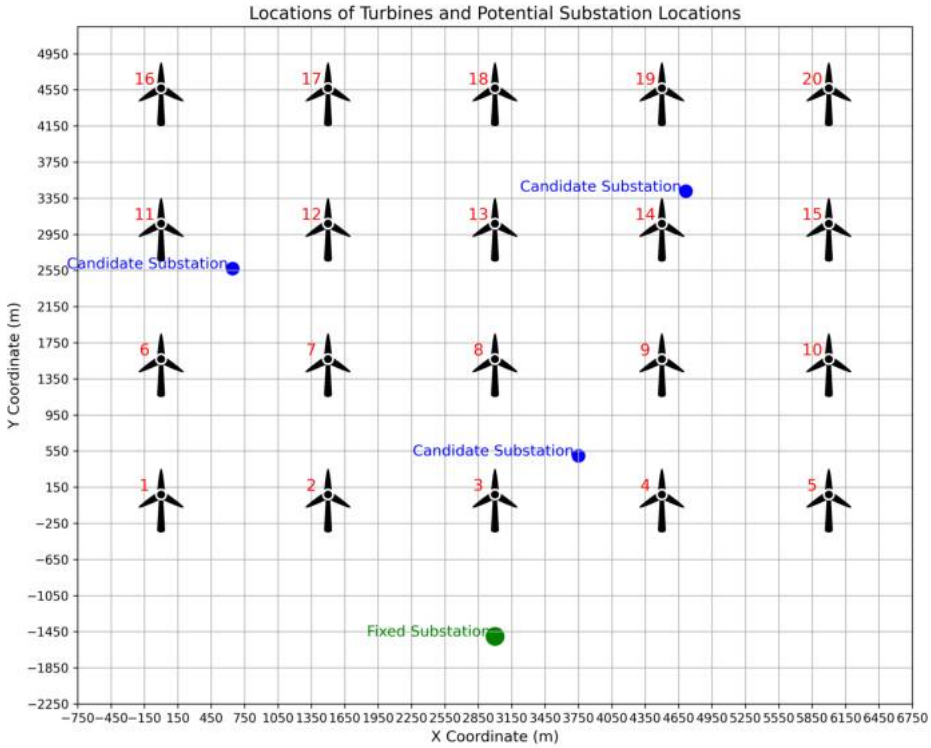

Figure 4.1: Locations of Turbines and the Fixed and Clustering-based Candidate Offshore Substation Locations

The Figure 4.1 illustrates the layout of the turbines and the fixed and clustering-based candidate offshore substation locations. Also, the candidate locations for offshore substation based on the clustering results are separately depicted in Figure 4.2 to show which turbines are in a same cluster based on the their coordinates. Additionally, Figure 4.3 depicts the PCC location, considering the positions of the turbines and the fixed and clustering-based candidate offshore substations. The turbines are arranged in a grid with a regular spacing to optimize wind capture and minimize wake effects. The offshore substation locations are positioned to minimize the total length of the medium-voltage cables connecting the turbines. The high-voltage cables connect the substation to the PCC onshore to complete the power transmission path.

4.2 Mathematical Formulations: Objective Function and Technical Constraints

This part provides the formulations and constraints for the proposed optimization model.

4.2.1 Nomenclature

Index Sets

T Turbines, indexed by i, j

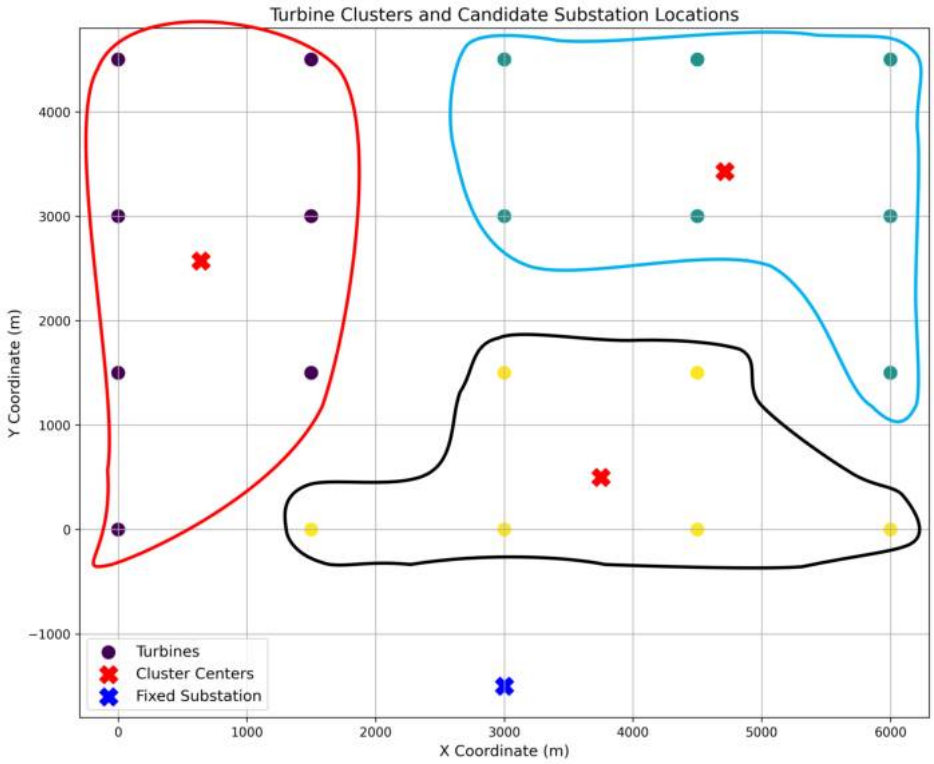

Figure 4.2: Locations of Turbines and the Fixed and Clustering-based Candidate Offshore Substation Locations

D Days in the optimization horizon, indexed by d

H Hours in a day, indexed by e

K_{MV} Medium voltage (MV) AC cable types, indexed by k

K_{HV} High voltage (HV) AC cable types, indexed by h

P_{HV} Possible HVAC cable paths, indexed by hp

DC High voltage direct current (HVDC) cable types, indexed by dc

T_{TR} Transformer types, indexed by t

P_{TR} Possible transformer positions, indexed by tp

L Offshore substation candicate locations, indexed by l

G Tangent lines for linearizing losses, indexed by g

Parameters

C_k Cost of MV cables per MW per meter (euro/MW/meter)

C_h Cost of HVAC cables per MW per meter (euro/MW/meter)

C_t Cost of transformers (euro/MW)

C_{dc} Cost of HVDC cable per MW per meter (euro/MW/meter)

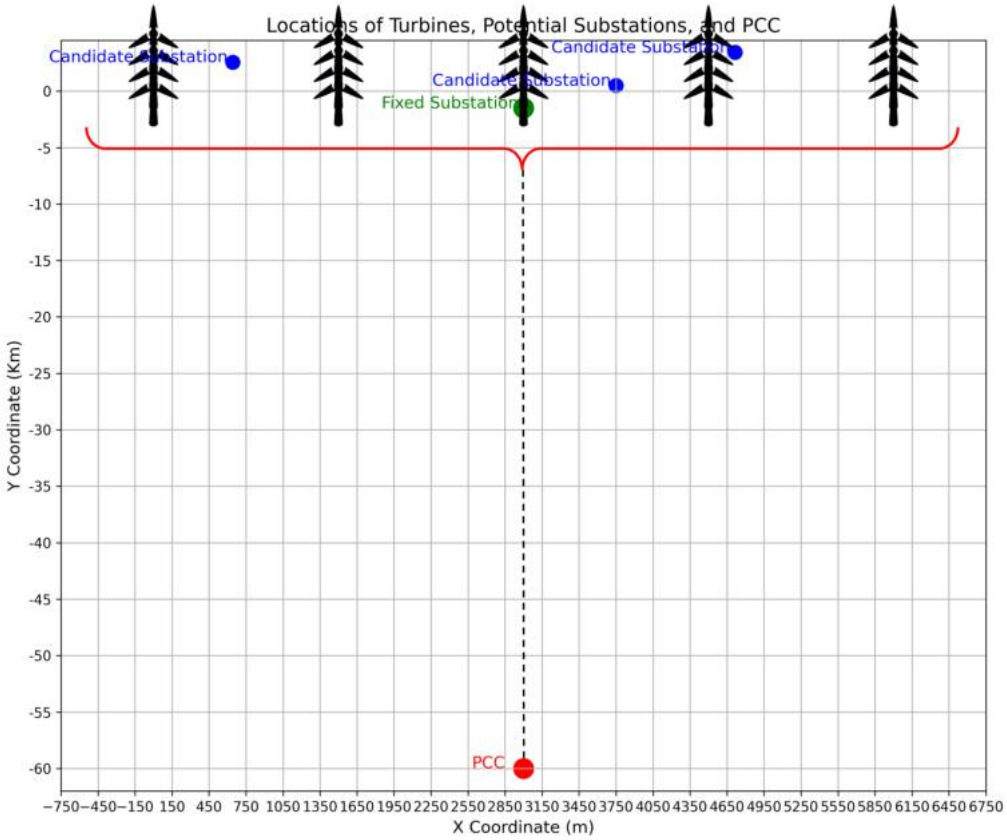

Figure 4.3: Locations of Turbines, Fixed and Clustering-based Candidate Offshore Substation Locations, and PCC

CV Cost of all required Voltage Source Converters (VSCs) for one HVDC corridor (euro/MW)

C_{loss} Cost of losses/wind energy curtailment or non-served energy (euro/MWh)

$HP_{d,e}$ Hourly market prices of energy for each day (euro/MWh)

ρ_d Weight of each representative day for calculating the total operation cost

V_{MV} Rated voltage for MV cables (kV)

V_{HV} Rated voltage for HVAC cables (kV)

V_{HVDC} Rated voltage of HVDC (kV)

RC_k Resistance of MV cables (ohm/m)

RC_h Resistance of HVAC cables (ohm/m)

R_{dc} Resistance of HVDC cables (ohm/m)

F_k Power rating of MV cables (MW)

F_h Power rating of HVAC cables (MW)

F_{dc} Power rating of HVDC cables (MW)

F_t Transformer rated power (MW)

PV^{max} VSC rated power (MW)

$D_{i,j}$ Distance matrix between turbines (i, j) (meter)

$D_{i,l}^{Sub}$ Distance between turbines *i* and offshore substation location *l* (meter)

D_{l}^{PCC} Distance between offshore substation location *l* and point of common coupling (PCC) (meter)

λ Total allowed number of offshore substations

I Interest rate

LT Lifetime of the offshore wind farm (years)

β Coefficient representing linear losses in VSC (conduction losses in semiconductors) (Ω)

γ Coefficient representing quadratic losses in VSC (switching losses) (Kv)

$\pi_{i,j,k,d,e,g}^{P}$ Parameter for linearizing losses in MV cables between turbines

$\pi_{i,k,l,d,e,g}^{Q}$ Parameter for linearizing losses in MV cables from each turbine to each offshore substation candidate location

$\pi_{h,p,l,d,e,g}^{R}$ Parameter for linearizing losses in HVAC cables between offshore substation candidate locations and the PCC

$\pi_{dc,l,d,e,g}^{PV^{ACside}}$ Parameter for linearizing losses in VSC (during converting AC to DC) in offshore substation candidate locations

$\pi_{dc,l,d,e,g}^{PV^{DCside}}$ Parameter for linearizing losses in HVDC cables and VSC (during converting DC to AC) in PCC

Variables

$Y_{i,j,k}$ Binary variable for MV cables between turbines

$Z_{i,k,l}$ Binary variable for MV cables between each turbine and each offshore substation candidate location

$W_{h,hp,l}$ Binary variable for HVAC cables between offshore substation candidate locations and PCC

$X_{l,t,tp}$ Binary variable for transformer installation at each offshore substation candidate location

S_{l} Binary variable for offshore substation location selection

$YD_{dc,l}$ Binary variable for HVDC cables between offshore substation candidate locations and PCC

$P_{i,j,k,d,e}$ Hourly power flow through MV cables between turbines (MW)

$Q_{i,k,l,d,e}$ Hourly power flow through MV cables from each turbine to each offshore substation candidate location (MW)

$R_{h,hp,l,d,e}$ Hourly power flow through HVAC cables from each offshore substation candidate location to PCC (MW)

$WC_{i,d,e}$ Hourly non-served energy or wind curtailment (MW)

$PV^{ACside}_{dc,l,d,e}$ Hourly power flow on the AC side of VSC in offshore substation in location *l* through HVDC cables to PCC (MW)

$PV^{DCside}_{dc,l,d,e}$ Hourly power flow on the DC side of VSC in offshore substation in location *l* through HVDC cables to PCC (MW)

$\Psi^{P}_{i,j,k,d,e}$ Variable for linearizing losses in MV cables between the turbines

$\Psi^{Q}_{i,k,l,d,e}$ Variable for linearizing losses in MV cables from each turbine to each offshore substation candidate location

$\Psi^{R}_{h,hp,l,d,e}$ Variable for linearizing losses in HVAC cables between offshore substation candidate locations and the PCC

$\Psi^{PV^{ACside}}_{dc,l,d,e}$ Variable for linearizing losses in VSC (during converting AC to DC) in offshore substation candidate locations

$\Psi^{PV^{DCside}}_{dc,l,d,e}$ Variable for linearizing losses in HVDC cables and VSC (during converting DC to AC) in PCC

4.2.2 Objective Function

The objective is to minimize the total cost, including both investment and operational costs, and to maximize the revenue from selling power at the PCC location:

$$\min \quad \textbf{Investment Cost} + \textbf{Operation Cost} - \textbf{Revenue} \tag{4.1}$$

4.2.2.1 Investment Cost

The total investment cost includes the costs of MV cables (both between turbines and between turbines and the offshore substation), HV AC and DC cables, transformers, and VSCs. This cost is adjusted by the capital recovery factor (CRF) to account for the interest rate and the lifetime of the wind farm, resulting in an equivalent annual investment cost as described in (4.2):

$$\begin{aligned}\textbf{Investment Cost} = \Bigg(& \sum_{i\in T}\sum_{j\in T}\sum_{k\in K_{MV}} Y_{i,j,k} D_{i,j} C_k F_k \\ & + \sum_{i\in T}\sum_{k\in K_{MV}}\sum_{l\in L} Z_{i,k,l} D^{Sub}_{i,l} C_k F_k \\ & + \sum_{h\in K_{HV}}\sum_{hp\in P_{HV}}\sum_{l\in L} W_{h,hp,l} D^{PCC}_{l} C_h F_h \\ & + \sum_{l\in L}\sum_{t\in T_{TR}}\sum_{tp\in P_{TR}} X_{l,t,tp} C_t F_t \\ & + \sum_{dc\in DC}\sum_{l\in L} (D^{PCC}_{l} C_{dc} F_{dc} + CV \cdot PV^{max}) Y D_{dc,l} \Bigg) \cdot \frac{I\cdot(1+I)^{LT}}{(1+I)^{LT}-1}\end{aligned} \tag{4.2}$$

4.2.2.2 Operational Cost & Revenue

The total operational cost is calculated for the entire year considering several representative days. Representative days are extracted from historical data using hierarchical clustering [29], which preserves the correlations between different feature vectors, such as wind data and market prices. As given by (4.3), the total operational cost includes the losses in MV cables, HV AC and DC cables, VSC, and wind curtailment costs.

$$\begin{aligned}\textbf{Operation Cost} = \sum_{d\in D}\rho_d \cdot \sum_{e\in H}\Big(&\textbf{Loss Cost (MV)}_{\textbf{d,e}} + \textbf{Loss Cost (To Offshore Substation)}_{\textbf{d,e}} \\ &+ \textbf{Loss Cost (HVAC)}_{\textbf{d,e}} + \textbf{Loss Cost (HVDC)}_{\textbf{d,e}} + \textbf{Loss Cost (VSC)}_{\textbf{d,e}} \\ &+ \textbf{Wind Curtailment Cost}_{\textbf{d,e}}\Big)\end{aligned} \tag{4.3}$$

Loss Costs: The hourly loss costs account for the energy losses in MV cables between turbines and from turbines to the offshore substation locations, HVAC cables, HVDC cables, and VSC:

$$\textbf{Loss Cost (MV)}_{\textbf{d,e}} = \sum_{i\in T}\sum_{j\in T}\sum_{k\in K_{MV}} 3\cdot\frac{\Psi^{P}_{i,j,k,d,e}}{(\sqrt{3}\cdot V_{MV})^2}\cdot RC_k\cdot D_{i,j}\cdot C_{\text{loss}} \tag{4.4}$$

$$\textbf{Loss Cost (To Offshore Substation)}_{\textbf{d,e}} = \sum_{i\in T}\sum_{k\in K_{MV}}\sum_{l\in L} 3\cdot\frac{\Psi^{Q}_{i,k,l,d,e}}{(\sqrt{3}\cdot V_{MV})^2}\cdot RC_k\cdot D^{Sub}_{i,l}\cdot C_{\text{loss}} \tag{4.5}$$

$$\textbf{Loss Cost (HVAC)}_{\textbf{d,e}} = \sum_{h\in K_{HV}}\sum_{hp\in P_{HV}}\sum_{l\in L} 3\cdot\frac{\Psi^{R}_{h,hp,l,d,e}}{(\sqrt{3}\cdot V_{HV})^2}\cdot RC_h\cdot D^{PCC}_{l}\cdot C_{\text{loss}} \tag{4.6}$$

$$\textbf{Loss Cost (HVDC)}_{\textbf{d,e}} = \sum_{dc\in DC}\sum_{l\in L}\frac{\Psi^{PV^{DCside}}_{dc,l,d,e}}{V^2_{HVDC}}\cdot R_{dc}\cdot D^{PCC}_{l}\cdot C_{\text{loss}} \tag{4.7}$$

$$\begin{aligned}\textbf{Loss Cost (VSC)}_{\textbf{d,e}} = &\sum_{dc\in DC}\sum_{l\in L}\Big(\beta\cdot(\frac{PV^{ACside}_{dc,l,d,e}}{V_{HVDC}}) + \gamma\cdot(\frac{\Psi^{PV^{ACside}}_{dc,l,d,e}}{{V_{HVDC}}^2}\Big)\cdot C_{\text{loss}} \\ &+ \sum_{dc\in DC}\sum_{l\in L}\Big(\beta\cdot(\frac{PV^{DCside}_{dc,l,d,e}}{V_{HVDC}}) + \gamma\cdot(\frac{\Psi^{PV^{DCside}}_{dc,l,d,e}}{{V_{HVDC}}^2})\Big)\cdot C_{\text{loss}}\end{aligned} \tag{4.8}$$

Note that, for simplicity, and since the losses in the collection grid configuration are lower than those in the transmission cables, this project disregards collection grid losses. Therefore, only the losses in HVAC and HVDC cables, as well as the losses in VSCs, are considered.

Wind Curtailment Cost: The hourly wind curtailment cost is the cost associated with the non-served energy:

$$\textbf{Wind Curtailment Cost}_{\textbf{d,e}} = \sum_{i\in T} WC_{i,d,e}\cdot C_{\text{loss}} \tag{4.9}$$

The total annual revenue, based on the operation of extracted representative days, is determined by calculating the product of the hourly prices and the power flow through the HVAC cables, subtracting the corresponding losses. It further includes the power flow through the HVDC cables, adjusted for losses within the HVDC system, which account for the HVDC cable and one VSC at the end of the cable for converting DC to AC. The VSC losses during AC-to-DC conversion are already included in the HVDC cable losses, as described in (4.20). The complete formulation is presented in (4.10):

$$\textbf{Revenue} = \sum_{d\in D} \rho_d \cdot \sum_{e\in H} \cdot \text{HP}_{d,e} \Bigg(\sum_{h\in K_{HV}} \sum_{hp\in P_{HV}} \sum_{l\in L} \Big(R_{h,hp,l,d,e} - \frac{3\cdot \Psi^{R}_{h,hp,l,d,e}}{(\sqrt{3}\cdot V_{HV})^2} \cdot RC_h \cdot D_l^{PCC} \Big) + \sum_{dc\in DC} \sum_{l\in L} \Big(PV^{DCside}_{dc,l,d,e} - \Big(\beta \cdot (\frac{PV^{DCside}_{dc,l,d,e}}{V_{HVDC}}) + \gamma \cdot (\frac{\Psi^{PV^{DCside}}_{dc,l,d,e}}{{V_{HVDC}}^2}) \Big) - \frac{\Psi^{PV^{DCside}}_{dc,l,d,e}}{V^2_{HVDC}} \cdot R_{dc} \cdot D_l^{PCC} \Big) \Bigg) \tag{4.10}$$

4.2.3 Constraints

4.2.3.1 Calculation of Power Output of Turbines (POT)

The hourly power output of each turbine ($POT_{i,d,e}$) is calculated based on the available data. Two methods are considered for this calculation, depending on the input dataset:

1. **Using Wind Speed and Direction Data:** When historical data of wind speed and wind direction is available, the calculation follows these steps:
   a) **Data Acquisition:** The wind speed and wind direction data for each hour of operation are obtained from the input dataset. These environmental conditions influence the power output of the turbines.
   b) **Power Curve:** Each turbine has a power curve provided by the manufacturer, which defines its power output as a function of wind speed and wind direction. For this study, we use the power curve data of a 4 GW wind farm located at IJmuiden Ver in the Netherlands, consisting of 204 turbines, each with a 20 MW capacity and a rotor diameter of 276 meters [30].
   c) **Interpolation:** To calculate the precise power output for given wind conditions, an interpolation method is applied. The *RegularGridInterpolator* from the SciPy library performs linear interpolation over the power curve data. Wind speeds and directions are used as independent variables, with power output as the dependent variable. Before interpolation, wind speed and direction values are clipped to ensure they fall within the valid range of the data.

   The resulting interpolated power value is scaled by the turbine's maximum power capacity (typically in MW), providing the final power output for each turbine at each hour.
2. **Using Historical Output Power Data:** If historical wind farm output power data is directly available, the wind factor (a measure of the effective power output as a proportion of the turbine's maximum capacity) can be calculated without requiring wind speed or direction data. The hourly wind farm output power data is divided by the total installed capacity of the farm to derive the wind factor. This factor is then scaled by the capacity of individual turbines to estimate the power output for each turbine at each hour.

Both methods ensure the accurate representation of dynamic power generation based on historical wind conditions. The calculated power output for each turbine at each hour ($POT_{i,d,e}$) is stored to meet the power balance constraints and support further optimization analysis. Note that for both methods, hierarchical clustering [29] is employed to extract representative data while preserving the correlations between different feature vectors, such as wind data and market prices.

4.2.3.2 Power Balance Constraint

The power balance constraint presented in (4.11) ensures that the power generated by each turbine (i.e., $POT_{i,d,e}$) plus the incoming power from other turbines equals the outgoing power plus the curtailed power. This is essential for maintaining the power balance at each turbine node for every day and hour.

$$\begin{aligned} POT_{i,d,e} + \sum_{j \in T} \sum_{k \in K_{MV}} \left(P_{j,i,k,d,e} - \frac{3 \cdot \Psi^{P}_{j,i,k,d,e}}{(\sqrt{3} \cdot V_{MV})^2} \cdot RC_k \cdot D_{j,i} \right) = \\ \sum_{j \in T} \sum_{k \in K_{MV}} P_{i,j,k,d,e} + \sum_{k \in K_{MV}} \sum_{l \in L} Q_{i,k,l,d,e} + WC_{i,d,e} \quad \forall i \in T, d \in D, e \in H \end{aligned} \tag{4.11}$$

where:

- $POT_{i,d,e}$ is the power output of turbine i during day d and hour e.
- $P_{j,i,k,d,e}$ minus the associated losses is the received power flow to turbine i from turbine j through medium voltage cable type k during day d and hour e.
- $P_{i,j,k,d,e}$ represents the power flow sent from turbine i to turbine j through medium voltage cable type k during day d and hour e.
- $Q_{i,k,l,d,e}$ is the power flow sent from turbine i to the offshore substation location l through medium voltage cable type k during day d and hour e.
- $WC_{i,d,e}$ is the wind curtailment (non-served energy) for turbine i during day d and hour e.

4.2.3.3 Offshore Substation Power Balance Constraint

This constraint ensures that the hourly power flow received in each offshore substation equals the power flow sent to the PCC, through HVAC or HVDC cables, as given by (4.12):

$$\begin{aligned} \sum_{i \in T} \sum_{k \in K_{MV}} \left(Q_{i,k,l,d,e} - \frac{3 \cdot \Psi^{Q}_{i,k,l,d,e}}{(\sqrt{3} \cdot V_{MV})^2} \cdot RC_k \cdot D^{Sub}_{i,l} \right) = \sum_{h \in K_{HV}} \sum_{hp \in P_{HV}} R_{h,hp,l,d,e} \\ + \sum_{dc \in DC} PV^{ACside}_{dc,l,d,e} \quad \forall l \in L, d \in D, e \in H \end{aligned} \tag{4.12}$$

4.2.3.4 Wind Curtailment Limit

This constraint ensures that the hourly wind curtailment at each turbine does not exceed the generated power as:

$$WC_{i,d,e} \leq POT_{i,d,e} \quad \forall i \in T, d \in D, e \in H \tag{4.13}$$

4.2.3.5 Total Transferred Power Constraint

The constraint presented by (4.14) limits the total power transferred to the PCC through HVAC cables by the transformer capacity:

$$\sum_{h \in K_{HV}} \sum_{hp \in P_{HV}} R_{h,hp,l,d,e} \leq \sum_{t \in T_{TR}} \sum_{tp \in P_{TR}} X_{l,t,tp} \cdot F_t \quad \forall l \in L, d \in D, e \in H \tag{4.14}$$

4.2.3.6 Power Flow Constraints

These constraints limit the power flow through all cables to their respective power capacities considering the related losses:

$$P_{i,j,k,d,e} + \frac{3 \cdot \Psi^{P}_{i,j,k,d,e}}{(\sqrt{3} \cdot V_{MV})^2} \cdot RC_k \cdot D_{i,j} \leq F_k \cdot y_{i,j,k} \quad \forall i,j \in T, k \in K_{MV}, d \in D, e \in H \tag{4.15}$$

The constraint (4.15) indicates that the power flow through each installed MV cable between turbines considering the related losses should be less than or equal to the maximum power limit of that cable (if it is installed).

$$Q_{i,k,l,d,e} + \frac{3 \cdot \Psi^{Q}_{i,k,l,d,e}}{(\sqrt{3} \cdot V_{MV})^2} \cdot RC_k \cdot D^{Sub}_{i,l} \leq F_k \cdot z_{i,k,l} \quad \forall i \in T, k \in K_{MV}, l \in L, d \in D, e \in H \tag{4.16}$$

The constraint (4.16) ensures that the power flow through each MV cable between each turbine and each offshore substation location considering the related losses does not exceed the maximum power limit of that cable (if it is installed).

$$R_{h,hp,l,d,e} + \frac{3 \cdot \Psi^{R}_{h,hp,l,d,e}}{(\sqrt{3} \cdot V_{HV})^2} \cdot RC_h \cdot D^{PCC}_{l} \leq F_h \cdot w_{h,hp} \quad \forall h \in K_{HV}, hp \in P_{HV}, l \in L, d \in D, e \in H \tag{4.17}$$

The power flow through each installed HVAC cable between each offshore substation location and the PCC considering the related losses is limited by constraint (4.17).

$$PV^{DCside}_{dc,l,d,e} + \frac{\Psi^{PV^{DCside}}_{dc,l,d,e}}{V^2_{HVDC}} \cdot R_{dc} \cdot D^{PCC}_{l} \leq F_{dc} \cdot YD_{dc,l} \quad \forall dc \in DC, l \in L, d \in D, e \in H \tag{4.18}$$

Finally, the power flow through HVDC cables between each offshore substation location and the PCC considering the related losses is limited by constraint (4.18).

4.2.3.7 VSC Coupling Constraints

In this project, a VSC-based HVDC transmission system is modeled, with power losses in both VSCs and the HVDC cable taken into account. The structure of the modeled VSC-based HVDC transmission system is depicted in Figure 4.4. The power losses for each VSC are calculated as follows [31, 32]:

$$Loss^{HVDC}_{dc,l,d,e} = \alpha + \beta(\frac{P^{Input}_{dc,l,d,e}}{V_{HVDC}}) + \gamma(\frac{(P^{Input}_{dc,l,d,e})^2}{{V_{HVDC}}^2}) \quad \forall dc \in DC, l \in L, d \in D, e \in H \tag{4.19}$$

In (4.19), the parameter α, representing the constant losses (standby, control, cooling), is negligible and can be ignored.

To account for the HVDC power coupling on both the AC and DC sides of each VSC while considering VSC losses, the coupling constraint (4.20) is defined. This constraint specifies that the power on the DC side equals the power on the AC side, reduced by the VSC power losses:

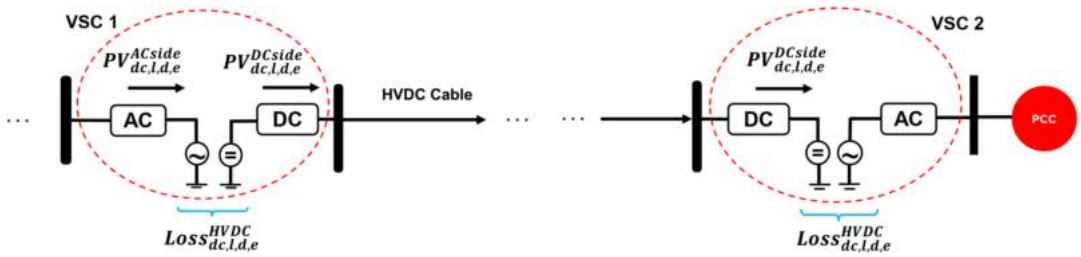

Figure 4.4: Structure of the VSC-Based HVDC Transmission System, Including VSCs, HVDC Cable, and PCC

$$PV^{DCside}_{dc,l,d,e} = PV^{ACside}_{dc,l,d,e} - \left(\beta \cdot (\frac{PV^{ACside}_{dc,l,d,e}}{V_{HVDC}}) + \gamma \cdot (\frac{\Psi^{PV^{ACside}}_{dc,l,d,e}}{{V_{HVDC}}^2}) \right) \quad \forall dc \in DC, l \in L, d \in D, e \in H \tag{4.20}$$

4.2.3.8 Transformer and Cable Type Constraints

The constraint (4.21) specifies that only one transformer type can be installed at each transformer position. Constraints (4.22) to (4.24) ensure that only one cable type is used for each connection. Additionally, each turbine i can only be connected either to another turbine or to the offshore substation location to keep the radial connection, as expressed in (4.25).

$$\sum_{t \in T_{TR}} X_{l,t,tp} \leq 1 \quad \forall tp \in P_{TR}, l \in L \tag{4.21}$$

$$\sum_{h \in K_{HV}} W_{h,hp,l} \leq 1 \quad \forall hp \in P_{HV}, l \in L \tag{4.22}$$

$$\sum_{k \in K_{MV}} Y_{i,j,k} \leq 1 \quad \forall i, j \in T \tag{4.23}$$

$$\sum_{k \in K_{MV}} Z_{i,k,l} \leq 1 \quad \forall i \in T, l \in L \tag{4.24}$$

$$\sum_{j \in T} \sum_{k \in K_{MV}} Y_{i,j,k,d} + \sum_{k \in K_{MV}} \sum_{l \in L} Z_{i,k,l} \leq 1 \quad \forall i \in T \tag{4.25}$$

4.2.3.9 Offshore Substation Location Constraints

The constraints (4.26) to (4.29) indicate the total allowed number of installed offshore substations and the connection between the selected location and all cables.

$$\sum_{l \in L} S_l \leq \lambda \tag{4.26}$$

$$Z_{i,k,l} \leq S_l \quad \forall i \in T, k \in K_{MV}, l \in L \tag{4.27}$$

$$W_{h,hp,l} \leq S_l \quad \forall h \in K_{HV}, hp \in P_{HV}, l \in L \tag{4.28}$$

$$YD_{dc,l} \leq S_l \quad \forall dc \in DC, l \in L \tag{4.29}$$

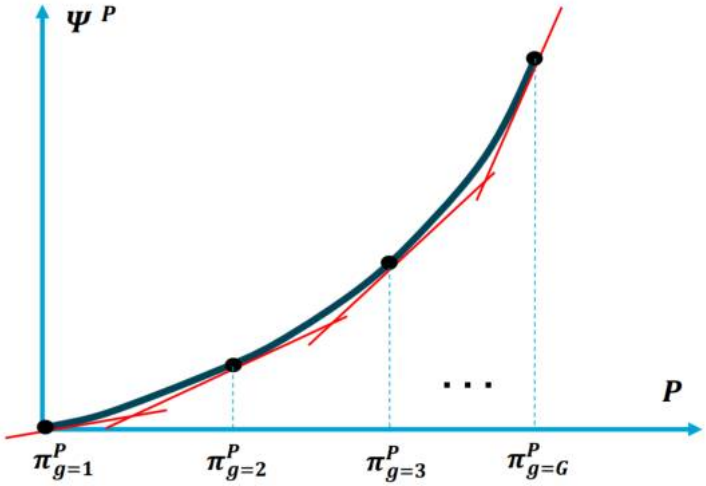

Figure 4.5: Utilized lower convex envelope method to linearize the squared power flow of cables

4.2.3.10Linearization of Cable Power Losses

The following constraints linearize the cable power losses using a lower convex envelope approximation [33]. The power losses in the cables are nonlinear in nature and can be complex to handle in optimization problems. To simplify the computation, we use a piecewise linear approximation, which is known as the lower convex envelope method. This method approximates the nonlinear loss functions by a series of linear segments.

The formulation involves auxiliary variables Ψ^P, Ψ^Q, and Ψ^R, which represent the linearized squared power flow of different types of cables to calculate the respective power losses. The auxiliary variables for HVDC systems are $\Psi^{PV^{ACside}}$ and $\Psi^{PV^{DCside}}$, which represent the squared power flow on the AC side and DC side of each VSC. The squared power flow of MV cables between different turbines can be approximated by a set of tangent lines, considering their slopes and contact points as given by (4.30). Figure 4.5 illustrates the concept of the utilized linearization methodology to linearize the squared power flow of cables (MV cables between the turbines as an example).

$$\Psi^P_{i,j,k,d,e} \geq P_{i,j,k,d,e} \cdot 2\pi^P_{i,j,k,d,e,g} - (\pi^P_{i,j,k,d,e,g})^2 \quad \forall i,j \in T, k \in K_{MV}, d \in D, e \in H, g \in G \tag{4.30}$$

The squared power flow of MV cables between each turbine and each offshore substation location is approximated by (4.31).

$$\Psi^Q_{i,k,l,d,e} \geq Q_{i,k,l,d,e} \cdot 2\pi^Q_{i,k,l,d,e,g} - (\pi^Q_{i,k,l,d,e,g})^2 \quad \forall i \in T, k \in K_{MV}, l \in L, d \in D, e \in H, g \in G \tag{4.31}$$

For HVAC cables between the offshore substation and PCC, the squared power flow is given by (4.32).

$$\Psi^R_{h,hp,l,d,e} \geq R_{h,hp,l,d,e} \cdot 2\pi^R_{h,hp,l,d,e,g} - (\pi^R_{h,hp,l,d,e,g})^2 \quad \forall h \in K_{HV}, hp \in P_{HV}, l \in L, d \in D, e \in H, g \in G \tag{4.32}$$

For HVDC cables and VSC, the squared power flow on the AC side and DC side of each VSC are given by (4.33) and (4.34).

$$\Psi_{dc,l,d,e}^{PV^{ACside}} \geq PV_{dc,l,d,e}^{ACside} \cdot 2\pi_{dc,l,d,e,g}^{PV^{ACside}} - (\pi_{dc,l,d,e,g}^{PV^{ACside}})^2 \quad \forall dc \in DC, l \in L, d \in D, e \in H, g \in G \tag{4.33}$$

$$\Psi_{dc,l,d,e}^{PV^{DCside}} \geq PV_{dc,l,d,e}^{DCside} \cdot 2\pi_{dc,l,d,e,g}^{PV^{DCside}} - (\pi_{dc,l,d,e,g}^{PV^{DCside}})^2 \quad \forall dc \in DC, l \in L, d \in D, e \in H, g \in G \tag{4.34}$$

The parameters $\pi_{i,j,k,d,e,g}^{P}$, $\pi_{i,k,l,d,e,g}^{Q}$, $\pi_{h,hp,l,d,e,g}^{R}$, $\pi_{dc,l,d,e,g}^{PV^{ACside}}$, and $\pi_{dc,l,d,e,g}^{PV^{DCside}}$, which are the contact points of the considered tangent lines, can be calculated as follows:

$$\pi_{i,j,k,d,e,g}^{P} = \frac{(g-1)}{(G-1)} \cdot F_k \quad \forall i, j \in T, k \in K_{MV}, d \in D, e \in H, g \in G \tag{4.35}$$

$$\pi_{i,k,l,d,e,g}^{Q} = \frac{(g-1)}{(G-1)} \cdot F_k \quad \forall i \in T, k \in K_{MV}, l \in L, d \in D, e \in H, g \in G \tag{4.36}$$

$$\pi_{h,hp,l,d,e,g}^{R} = \frac{(g-1)}{(G-1)} \cdot F_h \quad \forall h \in K_{HV}, hp \in P_{HV}, l \in L, d \in D, e \in H, g \in G \tag{4.37}$$

$$\pi_{dc,l,d,e,g}^{PV^{ACside}} = \frac{(g-1)}{(G-1)} \cdot F_{dc} \quad \forall dc \in DC, l \in L, d \in D, e \in H, g \in G \tag{4.38}$$

$$\pi_{dc,l,d,e,g}^{PV^{DCside}} = \frac{(g-1)}{(G-1)} \cdot F_{dc} \quad \forall dc \in DC, l \in L, d \in D, e \in H, g \in G \tag{4.39}$$

where:

- G is the total number of tangent lines used for the piecewise linear approximation.
- g is the index for the tangent lines, ranging from 1 to G.

By using these linearization constraints, we can approximate the nonlinear power loss functions with linear expressions, transforming the optimization problem into an MILP problem solvable using linear programming techniques. This approach significantly reduces computational complexity, which makes it feasible to solve large-scale optimization problems in the context of wind farm layout and cable installation design.

4.2.3.11 Avoid Inter-array Cable Crossings

Avoiding cable crossings in offshore wind farms is critical to reducing technical risks and economic impacts. This is important for medium-voltage (MV) inter-array cables between turbines, and between MV inter-array and high-voltage (HV) transmission cables. Cable crossings introduce significant installation challenges; the pressure and movement involved can weaken protective layers and increase the likelihood of faults and repairs. Economically, cable crossings demand extra protective measures like concrete mattresses or rock dumping, depending on site conditions. These requirements drive up installation costs further, compounded by the need for specialized vessels and crews. Delays can add tens of thousands of euros daily. Operationally, crossing points are highly vulnerable to seabed activities and anchoring which can lead to to repair expenses that may reach several million euros. Additionally, the stress at crossing points reduces cable lifespan. Optimal design strategies, such as avoiding cable crossings through efficient cable routing, can significantly enhance the reliability and cost-effectiveness of offshore wind farm operations [34, 35].

The designed constraints for avoiding cable crossings, employing a geometric technique [36], ensure that no two cables intersect. As mentioned, this is critical for reducing installation and maintenance costs while mitigating potential faults. The approach has been extended to address crossings not only between MV cables connecting turbines and linking turbines to offshore substation locations but also between MV cables and HVAC cables, as well as between MV cables and HVDC cables (i.e., MV interarray and HV transmission cables). This extension reflects the increasing complexity of offshore wind farm layouts.

To determine if two cables intersect, we use a geometric approach based on the orientations of the points (i.e., turbines, substation locations, and PCC). The orientation function determines the relative direction of three points in a 2D plane. Using this function, we can check if the line segments (i.e., cables) defined by these points intersect. If they do intersect, the defined constraints ensure that at most one of these segments is selected, thus avoiding crossings.

Orientation Function:

The orientation function calculates the relative direction of an ordered triplet of points (p, q, r) in a 2D plane. This direction is determined using the cross-product of vectors, as follows:

$$\text{val} = (y_q - y_p)(x_r - x_q) - (x_q - x_p)(y_r - y_q). \tag{4.40}$$

Based on the value of val:

- If val $= 0$, the points are collinear.
- If val > 0, the points are oriented clockwise.
- If val < 0, the points are oriented counterclockwise.

Intersection Check:

The intersection check determines if two line segments (p_1, q_1) and (p_2, q_2) intersect. This is achieved using the orientations of the points that define the segments. The steps are as follows:

1. Compute the orientations of the following ordered triplets:

$$o_1 = \text{orientation}(p_1, q_1, p_2), \quad o_2 = \text{orientation}(p_1, q_1, q_2),$$
$$o_3 = \text{orientation}(p_2, q_2, p_1), \quad o_4 = \text{orientation}(p_2, q_2, q_1).$$

2. The segments (p_1, q_1) and (p_2, q_2) intersect if and only if:

$$o_1 \neq o_2 \quad \text{and} \quad o_3 \neq o_4. \tag{4.41}$$

Constraints for Avoiding Cable Crossings

Using the orientation and intersection check functions, we define constraints to prevent cable crossings in offshore wind farm cable routing. These constraints address crossings not only between MV cables connecting turbines, but also between turbine-to-substation MV cables, HVAC and HVDC transmission cables.

1. **For MV ↔ MV Cables (Turbine-to-Turbine):** To ensure that two MV cables connecting turbines do not intersect, the constraint (4.42) is applied:

$$Y_{i,j,k} + Y_{ii,jj,k} \leq 1, \quad \forall i, j, ii, jj \in T,\, i < j,\, ii < jj,\, i \neq ii,\, j \neq jj,\, \forall k \in K_{MV} \tag{4.42}$$

   where:

   - $Y_{i,j,k}$ is a binary variable indicating whether an MV cable of type k is installed between turbine i and turbine j.
   - $Y_{ii,jj,k}$ is a binary variable indicating whether an MV cable of type k is installed between turbine ii and turbine jj.

2. **For MV (Turbine-to-Turbine) ↔ MV (Turbine-to-Substation):** To prevent intersections between MV cables connecting turbines and MV cables linking turbines to substations, the constraint (4.43) is defined:

$$Y_{i,j,k} + Z_{i,k,l} \leq 1, \quad \forall i, j \in T,\, i < j,\, \forall k \in K_{MV},\, \forall l \in L \tag{4.43}$$

   where:

   - $Z_{i,k,l}$ is a binary variable indicating whether an MV cable of type k is installed between turbine i and substation location l.

3. **For MV ↔ HVAC Cables:** To prevent intersections between MV cables and HVAC cables running between substations and the PCC, the following constraint is imposed:

$$Y_{i,j,k} + W_{h,hp,l} \leq 1, \quad \forall i, j \in T,\, i < j,\, \forall k \in K_{MV},\, \forall h \in K_{HV},\, \forall hp \in P_{HV},\, \forall l \in L \tag{4.44}$$

   Additionally, intersections between turbine-to-substation MV cables and HVAC cables are addressed using:

$$Z_{i,k,l} + W_{h,hp,l} \leq 1, \quad \forall i \in T,\, \forall k \in K_{MV},\, \forall h \in K_{HV},\, \forall hp \in P_{HV},\, \forall l \in L \tag{4.45}$$

4. **For MV ↔ HVDC Cables:** To ensure that MV cables do not intersect HVDC cables running between substations and the PCC, the following constraint is applied:

$$Y_{i,j,k} + YD_{dc,l} \leq 1, \quad \forall i, j \in T,\, i < j,\, \forall k \in K_{MV},\, \forall dc \in DC,\, \forall l \in L \tag{4.46}$$

   Additionally, intersections between turbine-to-substation MV cables and HVDC cables are addressed using:

$$Z_{i,k,l} + YD_{dc,l} \leq 1, \quad \forall i \in T,\, \forall k \in K_{MV},\, \forall dc \in DC,\, \forall l \in L \tag{4.47}$$

By employing a geometric approach based on orientation and intersection checks, we ensure that no two cables intersect in the offshore wind farm cable routing.

4.2.3.12Auxiliary Constraints

To accelerate the proposed optimization model, auxiliary constraints can be defined to reduce the model search space during the solving process.

Symmetry Breaking Constraint: To prevent redundant symmetrical solutions and ensure that there is at most one MV cable type connecting any two turbines, we define the constraint (4.48):

$$\sum_{k \in K_{MV}} Y_{i,j,k} + \sum_{k \in K_{MV}} Y_{j,i,k} \leq 1 \quad \forall i, j \in T, i \neq j \tag{4.48}$$

This constraint ensures that if there is an MV cable connecting turbine i to turbine j, there cannot be another MV cable connecting turbine j to turbine i. This helps to reduce the search space by eliminating symmetrical solutions.

Maximum Number of Cables from Turbine: To guarantee the radial connection between the turbines, constraint (4.49) is defined. This constraint ensures that each turbine i can connect to at most one other turbine through an MV cable. It also simplifies the network design and reduces the number of potential configurations the solver needs to evaluate.

$$\sum_{j \in T} \sum_{k \in K_{MV}} Y_{i,j,k} \leq 1 \quad \forall i \in T \tag{4.49}$$

Maximum Number of Transformers: To control costs and simplify the design of each offshore substation, we limit the number of transformers that can be installed by:

$$\sum_{t \in T_{TR}} \sum_{tp \in P_{TR}} X_{l,t,tp} \leq 2 \quad \forall l \in L \tag{4.50}$$

This constraint ensures that the total number of transformer types installed at all positions in each offshore substation does not exceed two. This helps control the investment cost and operational complexity of the substation.

Maximum Number of Cables to each Offshore Substation: This constraint limits the total number of connected cables from turbines to the offshore substation:

$$\sum_{i \in T} \sum_{k \in K_{MV}} Z_{i,k,l} \leq \alpha \quad \forall l \in L \tag{4.51}$$

In (4.51), α can be equal to the number of columns in turbines arrangement.

4.3 Mathematical Formulations: Ring Connection Configuration

The ring connection configuration links wind turbines in a circular pattern, which can create a closed loop as illustrated in Figure 3.2. This design increases system resilience by providing an alternate circuit for electricity if a failure occurs in any line or component. It simplifies maintenance and reduces the risk of total power failures. However, the increased reliability and flexibility come with higher complexity and cost.

In this section the required formulations and modifications to have a ring connection configuration are discussed.

To create a loop or ring connection the constraint (4.52) is defined:

$$\sum_{j \in T} \sum_{k \in K_{MV}} Y_{i,j,k} + \sum_{j \in T} \sum_{k \in K_{MV}} Y_{j,i,k} + \sum_{k \in K_{MV}} \sum_{l \in L} Z_{i,k,l} \geq 2 \quad \forall i \in T \tag{4.52}$$

The constraint (4.52) indicates that each turbine can be connected to at least two other turbines or one turbine and one offshore substation. This constraint ensures a loop or ring connection, providing redundancy and improving the reliability. Moreover, the constraint (4.49) need to be modified as follows:

$$\sum_{j \in T} \sum_{k \in K_{MV}} Y_{i,j,k} \leq 2 \quad \forall i \in T \tag{4.53}$$

Furthermore, the power flow constraint presented in (4.15) must be reformulated to enable bidirectional power transfer for each turbine. The revised constraint is expressed as follows:

$$P_{i,j,k,d,e} + \frac{3 \cdot \Psi^{P}_{i,j,k,d,e}}{(\sqrt{3} \cdot V_{MV})^2} \cdot RC_k \cdot D_{i,j} \leq F_k \cdot (y_{i,j,k} + y_{j,i,k}) \quad \forall i,j \in T,\, k \in K_{MV},\, d \in D,\, e \in H \tag{4.54}$$

The constraint in (4.54) ensures power transfer in both directions for each loop or ring.

Note that other constraints remain unchanged.

4.4 Mathematical Formulations: Star Connection Configuration

Within the star collection system, each WTG establishes a direct connection to a offshore substation via MV cables as illustrated in Figure 3.3. The star topology is renowned for its exceptional reliability. However, this topology is financially less attractive compared to other topologies. The required formulations and modifications to have a star connection configuration are discussed in the following. the constraint (4.25) should be replaced by (4.55).

$$\sum_{k \in K_{MV}} \sum_{l \in L} Z_{i,k,l} \leq 2 \quad \forall i \in T \tag{4.55}$$

Moreover, to guarantee the star connection the binary variables for inter-array connection between the turbines should be fixed to zero, as (4.56):

$$Y_{i,j,k} = 0 \qquad \forall i,j \in T, \forall k \in K_{MV} \tag{4.56}$$

The other required modification is changing α in (4.51) to be equal to the total number of turbines. The other constrains (4.11) to (4.24), and (4.26) to (4.50) remains unchanged.

5 Project Findings

5.1 Input Data

The described model is implemented in a case study with 20 wind turbines, arranged in 4 rows and 5 columns, each with a maximum power capacity of 20 MW. The distance between turbines in the same row and the distance between rows are considered to be 1500 meters, while the distance from the offshore location to the onshore PCC is assumed to be 60 kilometers. The rated voltages for the AC system are set to 66 kV for MV collection grid, and 220 kV for HV transmission system, while the rated voltage for the HVDC transmission system is set to 320 kV.

The wind curtailment cost (or non-served energy cost) is considered as 100 EUR/MWh. Two different types of cables are used for both MV and HV cables in the AC system, and one type of cable is used for the HVDC system. Detailed cable data is provided in Table 5.1. All MV and HV cable parameters are extracted from [37], while related investment costs are calculated based on [38, 39, 40, 41]. Cable lengths are calculated based on the relative positions of the turbines. The electrical resistances of the HV cables are calculated based on the resistivity of copper ($\rho = 1.68 \times 10^{-8}\ \Omega\cdot$m). Additionally, transformers of two types, rated at 200 MVA and 300 MVA, are considered for installation at either candidate or fixed offshore substation locations as reported in Table 5.2. Their respective cost, 0.19 million EUR/MW, is calculated based on a platform cost of 0.16 million EUR/MW and a substation cost of 0.03 million EUR/MW [42, 43, 44, 45].

For the HVDC system, one type of VSC with a rated power of 200 MW is considered, with a cost of 0.584 million EUR/MW [42, 45]. The coefficients β and γ used to calculate the VSC losses are 0.87 and 0.279 [32], as reported in Table 5.3. The HVDC cable parameters are extracted from [37], and its investment cost is calculated based on [39, 40] as presented in Table 5.1.

Note that the total number of tangent lines used for linearizing the cable and VSC losses is assumed to be 10 lines for computational efficiency.

Table 5.1: All Cable Parameters

Parameter	MVAC Cable	HVAC Cable	HVDC Cable
Cross-Sectional Area (mm^2)	95, 150	300, 800	240
Rated Power (MW)	34.29, 42.86	200, 295.31	200
Resistance (Ω/m)	Ignored	0.000056, 0.000021	0.000015
Investment Cost (EUR/m)	15.89	7.06	2.14
Voltage Rating (kV)	66	220	320

Table 5.2: HVAC Transformer Parameters

Parameter	Transformer Type 1	Transformer Type 2
Rated Power (MVA)	200	300
Cost (Million EUR/Unit)	38	57
Platform Cost (M€/MW)	0.16	0.16
Substation Cost (M€/MW)	0.03	0.03

Table 5.3: HVDC VSC Parameters

Parameter	Value	Unit
Rated Power	200	MW
Cost	0.1	Million EUR/MW
Platform Cost	0.268	Million EUR/MW
Substation Cost (Offshore)	0.268	Million EUR/MW
Topside Adjustment Cost	0.048	Million EUR/MW
Rated Voltage	320	kV
Linear Losses Coefficient (β)	0.87	kV
Quadratic Losses Coefficient (γ)	0.279	Ω

5.2 Extracted Representative Days

The market prices are obtained from the TYNDP Global Ambition scenario study for the 2030 perspective [46], while the weather data is sourced from [47]. Alternatively, historical data from [48] can be utilized to analyze both market prices and the power generated by offshore wind farms, providing a comprehensive overview of past trends and variations. Using hierarchical clustering [29], three representative days are extracted, with their respective cluster weights as shown in Table 5.4.

Table 5.4: Cluster Weights for Extracted Representative Days

Representative Day (Cluster)	Weight (days)
1	116
2	202
3	47
Total	**365**

Additionally, Figure 5.1 illustrates the wind factor in per unit (PU) across the representative days, while Figure 5.2 shows the corresponding market prices in EUR/MWh for the same representative days.

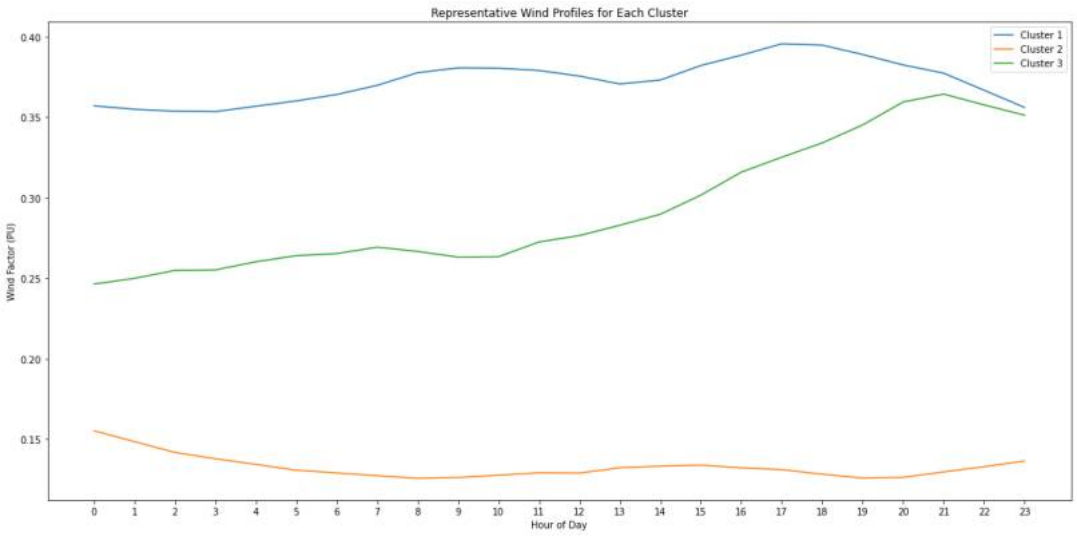

Figure 5.1: Wind Factor in PU Across Extracted Representative Days

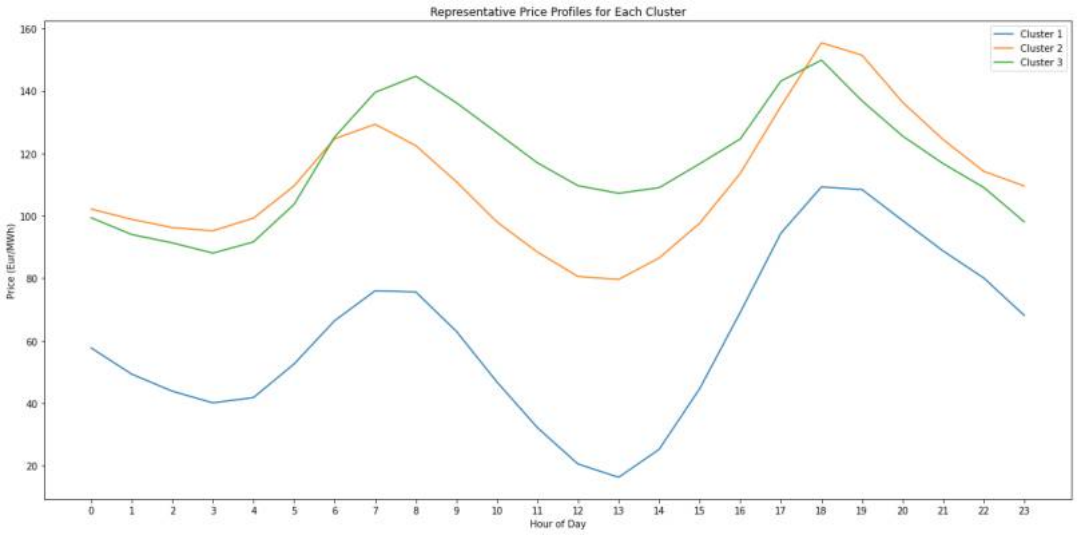

Figure 5.2: Market Prices in EUR/MWh Across Extracted Representative Days

5.3 Obtained Results

This section presents the simulation results for the collection grid and transmission system design along with sitting and sizing of offshore substations for the considered OWF. The analysis evaluates different cases to identify optimal designs and cost implications. The base case considers a Radial collection grid, focusing on achieving minimum cost and reliability. Alternative topologies, such as Ring and Star collection grids, are explored as the second and third cases. The study also examines the impact of multiple candidate locations for offshore substations on the final design and associated costs. Furthermore, the hybrid HVAC/HVDC transmission system is validated through scenario analysis, focusing on cases where the distance between the offshore substation and the PCC exceeds the break-even threshold of 80 km. Finally, a reliability assessment compares the operational reliability of radial, ring, and star configurations.

5.3.1 Base Case

The obtained results considering all the formulations (4.1) to (4.51) and the extracted representative days of operation with specific hourly wind factors, along with electricity market prices is presented in the following.

5.3.1.1 Obtained Results Considering a Fixed Offshore Substation Location

The simulation begins with the base case, which assumes a single fixed offshore substation location and incorporates cable crossing avoidance constraints. Figure 5.3 illustrates the layout of this case, highlighting the positions of the turbines and the fixed substation.

The obtained results for MV collection grid desig are reported in Table 5.5 and illustrated in Figure 5.4.

The MV cable connections between turbines are selected as 95 mm^2 cables (Type 1) based on the power requirements and cost optimization of the system. The 95 mm^2 cables provide sufficient capacity for power transfer while minimizing costs, making them an efficient and practical choice for the given layout.

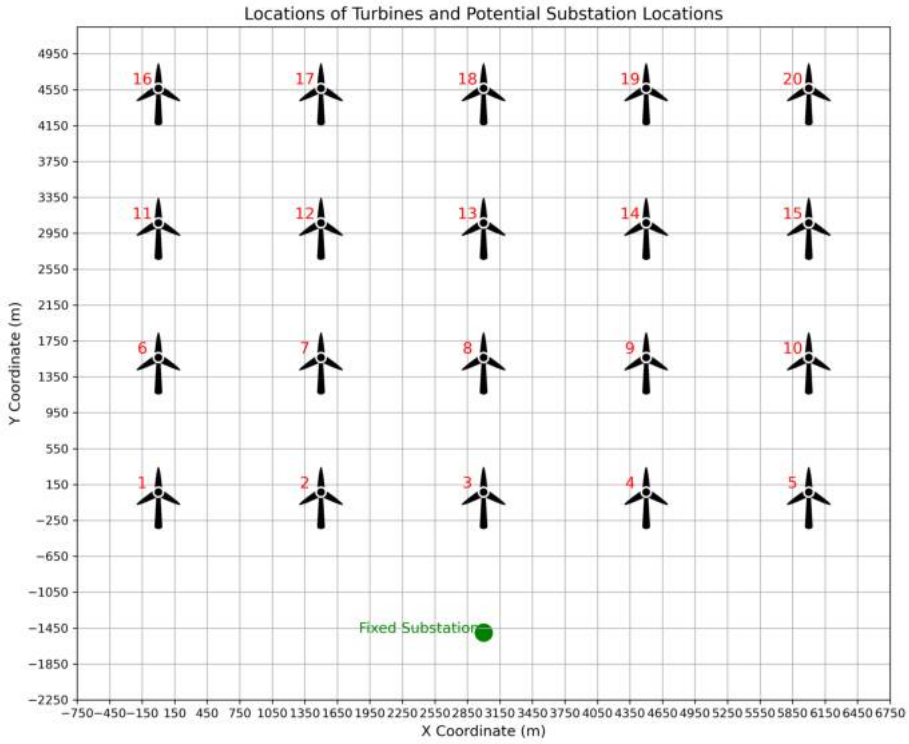

Figure 5.3: Layout of the Base Case with a Fixed Offshore Substation

Table 5.5: The Obtained Optimal MV Cable Connection Between the Turbines for Base Case with a Fixed Offshore Substation

From	To	MV Cable Type
6	1	95 mm^2
7	2	95 mm^2
8	3	95 mm^2
9	4	95 mm^2
10	5	95 mm^2
11	6	95 mm^2
12	7	95 mm^2
13	8	95 mm^2
14	9	95 mm^2
15	10	95 mm^2
16	11	95 mm^2
17	12	95 mm^2
18	13	95 mm^2
19	14	95 mm^2
20	15	95 mm^2

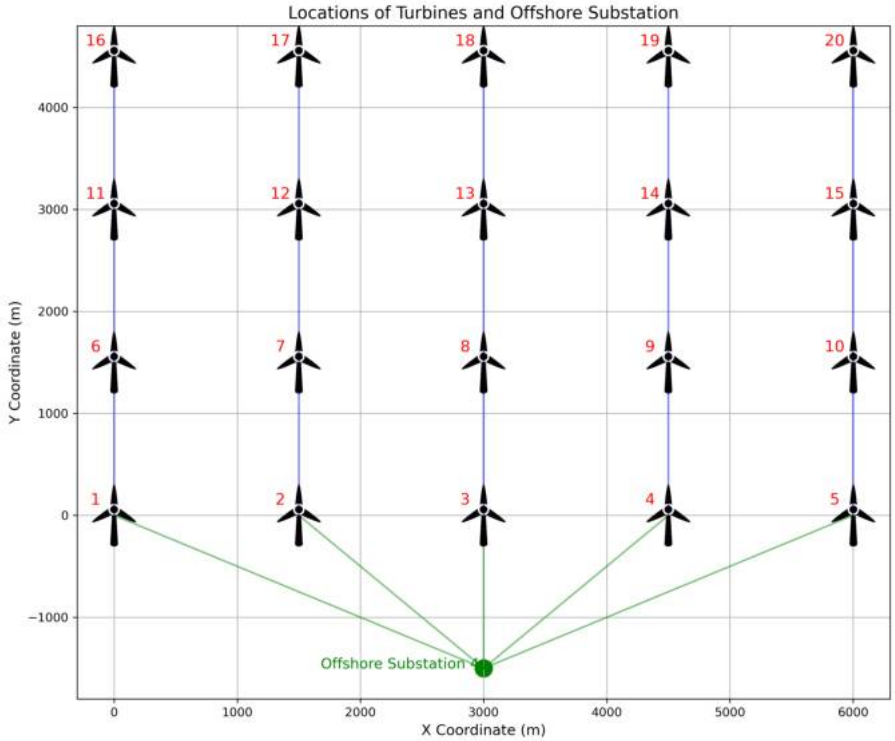

Figure 5.4: The Obtained Results Illustration for Base Case with a Fixed Offshore Substation

The MV cable connections between the turbines and the offshore substation are presented in Table 5.6. Each turbine is connected using 95 mm^2 cables (Type 1) to the fixed offshore substation.

Table 5.6: The Obtained Optimal MV Cable Connection Between the Turbines and the Fixed Offshore Substation for Base Case

Turbine	Type
1	95 mm^2
2	95 mm^2
3	95 mm^2
4	95 mm^2
5	95 mm^2

The fixed offshore substation is then connected to the PCC using an HVAC cable of Type 1, i.e., 300 mm^2, along path 1, as presented in Table 5.7 and illustrated in Figure 5.5.

Table 5.7: The Obtained Optimal HVAC Cable Connection Between the Fixed Offshore Substation and PCC for Base Case

Type	Path
300 mm^2	1

The only installed transformer in the offshore substation is of Type 1, with a capacity of 200

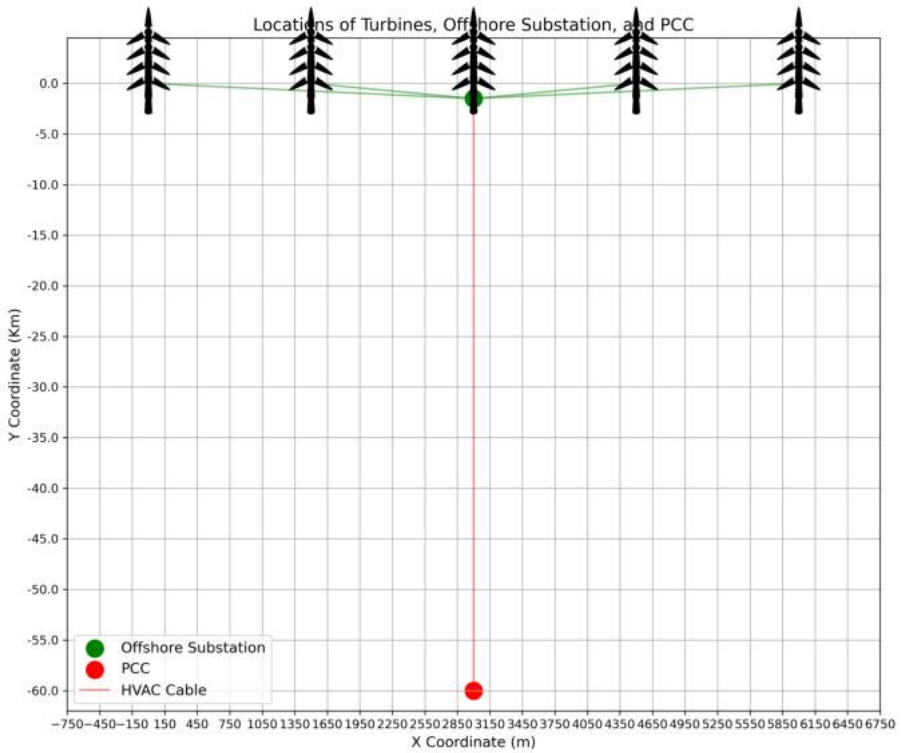

Figure 5.5: The Illustration of Connection Between Offshore Substation and PCC for Base Case with a Fixed Offshore Substation

MVA, as shown in Table 5.8.

Table 5.8: Installed Transformer Type and Position for Base Case with a Fixed Offshore Substation

Type	Position
200 MVA	1

The obtained costs, which encompass the total annualized investment cost of installed MV and HVAC cables also the transformer in offshore substation, total losses cost, wind energy curtailment cost, and total revenue, are detailed in Table 5.9.

In Figure 5.6, the average total power output, losses, and total delivered power across three representative days are illustrated for the base case scenario with a fixed offshore substation. The results highlight differences between the days, with representative day 1 demonstrating the highest average total power output and delivered power, while representative day 2 records the lowest. These variations correspond to the wind factor trends shown in Figure 5.1, reflecting the influence of environmental and operational conditions, such as wind speed fluctuations, on the offshore wind farm transmission system. The comparison of total delivered power and losses emphasizes the efficiency of the HVAC transmission system under different operational scenarios.

Table 5.9: The Obtained Costs of Investment and Operation along with Revenue for Base Case with a Fixed Offshore Substation

Total Cost & Revenue Component	Value (K€)
Annualized Investment Cost	10,275.37
Loss Cost (HV Cables)	615.96
Loss Cost (HVDC Cables)	0
Loss Cost (HVDC VSC)	0
Wind Curtailment Cost	0
Revenue from Energy Sales	69,055.38
Operation Cost	615.96
Revenue - Cost	58,164.05

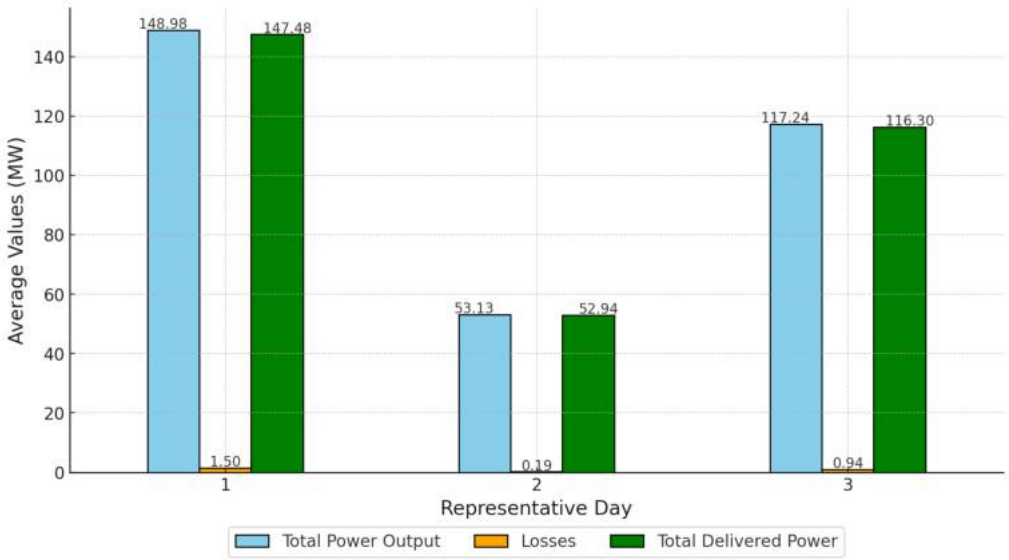

Figure 5.6: Illustration of Average Total Power Output, Losses, and Total Delivered Power per Representative Day for the Base Case with a Fixed Offshore Substation

5.3.1.2 Obtained Results Considering Multiple Candidate Offshore Substation Locations

This simulation evaluates multiple candidate offshore substation locations by integrating AI-driven clustering method and optimization techniques for substation selection. Figure 5.7 illustrates the layout for this scenario, showing turbine locations alongside candidate substation positions. The candidate locations were identified using hierarchical clustering [29], based on turbine coordinates, as depicted in Figure 4.2.

The results for the MV collection grid design are identical to the previous case, where only a fixed offshore substation was considered. These results are presented in Table 5.5 and visualized in Figure 5.4.

In the optimization process, the selected candidate substation corresponds to the fixed substation as also used in the previous case. The associated transformer type and position remain unchanged, as shown in Table 5.8.

Finally, the cost results for this case match those presented in Table 5.9.

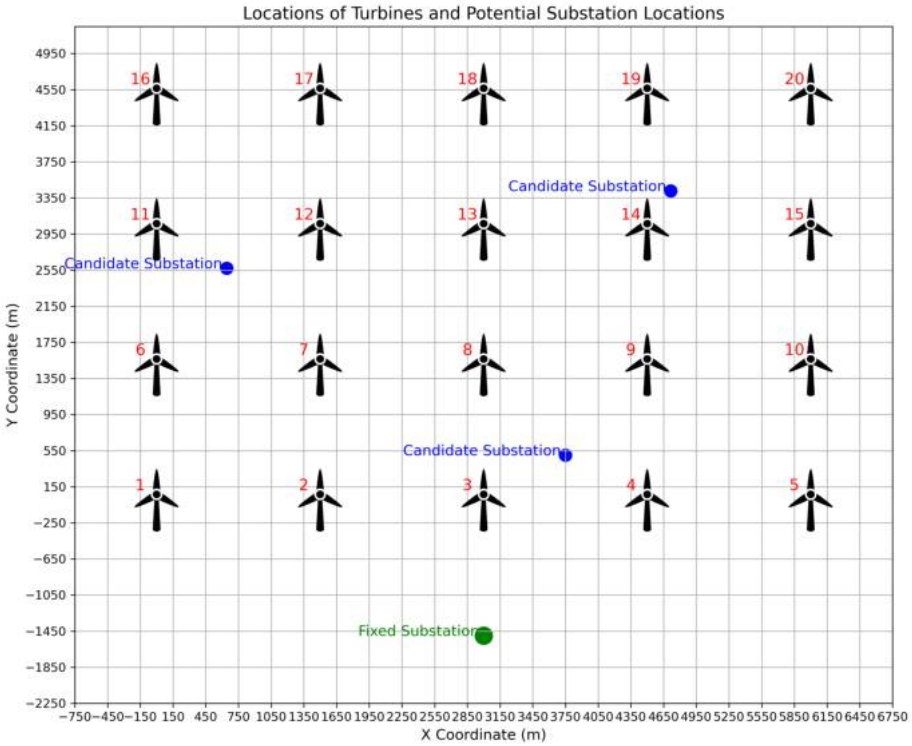

Figure 5.7: Layout of the Case with Multiple Candidate Offshore Substation Locations

5.3.2 Ring Connection Configuration

The obtained results considering the constraints (4.52), (4.53), and (4.54), to guarantee a ring connection configuration, are presented in this section.

5.3.2.1 Obtained Results Considering a Fixed Offshore Substation Location

The turbine locations and the fixed offshore substation location for the Ring Connection Configuration are identical to those shown in Figure 5.3. The obtained results for the MV collection grid design are illustrated in Figure 5.8.

The results for the MV cable connections between turbines are summarized in Table 5.10. As illustrated in Figure 5.8, the MV collection grid now adopts a ring configuration instead of the previously used radial connection. This ring configuration provides improved reliability by ensuring that power can flow in two directions, enhancing the robustness of the system against potential faults or failures in the cables. This design improves operational flexibility and ensures uninterrupted power transfer between turbines and the offshore substation.

The connections between turbines and the offshore substation are summarized in Table 5.11.

The fixed offshore substation is then connected to the PCC using an HVAC cable of Type 1 (300 mm^2), as shown in Table 5.12.

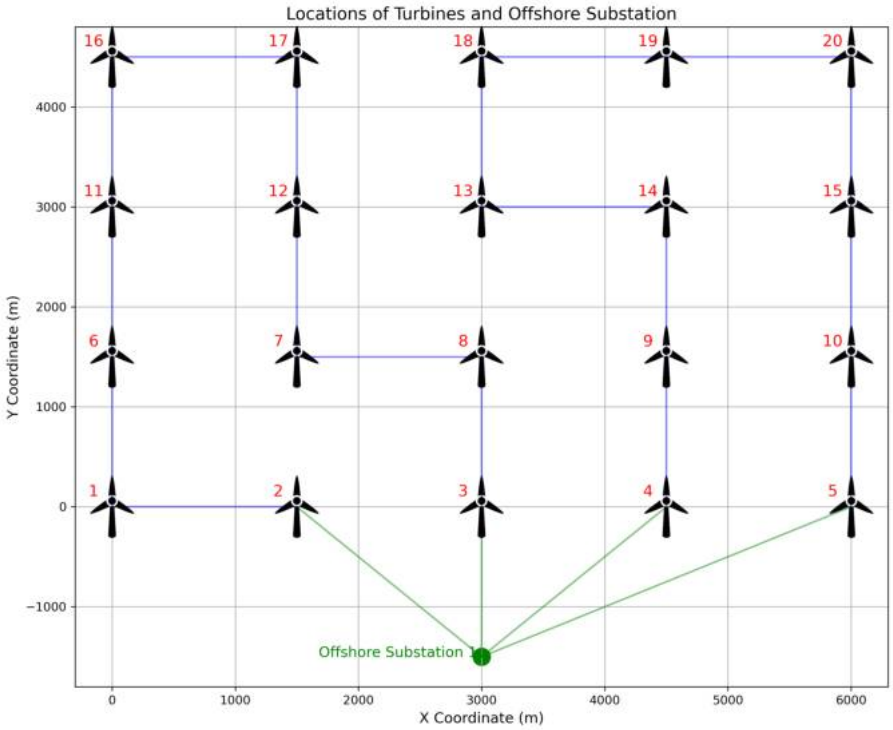

Figure 5.8: The Obtained Results Illustration for Ring Connection Configuration with a Fixed Offshore Substation Location

Table 5.10: The Obtained Optimal MV Cable Connection Between the Turbines for Ring Connection Configuration with a Fixed Offshore Substation Location

From	To	MV Cable Type
1	2	95 mm^2
6	1	95 mm^2
7	8	95 mm^2
8	3	95 mm^2
9	4	95 mm^2
10	5	95 mm^2
11	6	95 mm^2
12	7	95 mm^2
13	14	95 mm^2
14	9	95 mm^2
15	10	95 mm^2
16	11	95 mm^2
17	12	95 mm^2
17	16	95 mm^2
18	13	95 mm^2
19	18	95 mm^2
19	20	95 mm^2
20	15	95 mm^2

Table 5.11: The Obtained Optimal MV Cable Connection Between the Turbines and the Fixed Offshore Substation for Ring Connection Configuration

Turbine	MV Cable Type
2	150 mm^2
3	150 mm^2
4	150 mm^2
5	150 mm^2

Table 5.12: The Obtained Optimal HVAC Cable Connection Between the Fixed Offshore Substation and PCC for Ring Connection Configuration

HV Cable Type	Path
300 mm^2	1

The transformer installed in the fixed offshore substation is of Type 1, with a capacity of 200 MVA, as summarized in Table 5.13.

Table 5.13: Installed Transformer Type and Position for Ring Connection Configuration

Transformer Type	Position
200 MVA	1

The obtained costs, which include the total investment cost, total loss costs, wind curtailment cost, and total revenue, are detailed in Table 5.14.

Table 5.14: The Obtained Costs of Investment and Operation along with Revenue for Ring Connection Configuration with a Fixed Offshore Substation

Total Cost & Revenue Component	Value (K€)
Investment Cost	10,412.46
Loss Cost (HV Cables)	615.96
Loss Cost (HVDC Cables)	0
Loss Cost (HVDC VSC)	0
Wind Curtailment Cost	0
Revenue from Energy Sales	69,055.38
Operation Cost	615.96
Revenue - Cost	58,026.96

The total revenue minus cost for the ring connection configuration is 58,026.96 K€, compared to 58,164.05 K€for the radial connection (Base Case). This slight decrease in net revenue demonstrates that the higher reliability provided by the ring configuration comes at a marginally higher cost due to the additional cable lengths and redundancy required for the ring design. However, this trade-off enhances the system's robustness and operational flexibility.

5.3.2.2 Obtained Results Considering Multiple Candidate Offshore Substation Locations

The turbine positions and offshore substation candidate locations for this case are identical to those shown in Figure 5.7. The obtained results for the MV collection grid are summarized in Table 5.15 and illustrated in Figure 5.9.

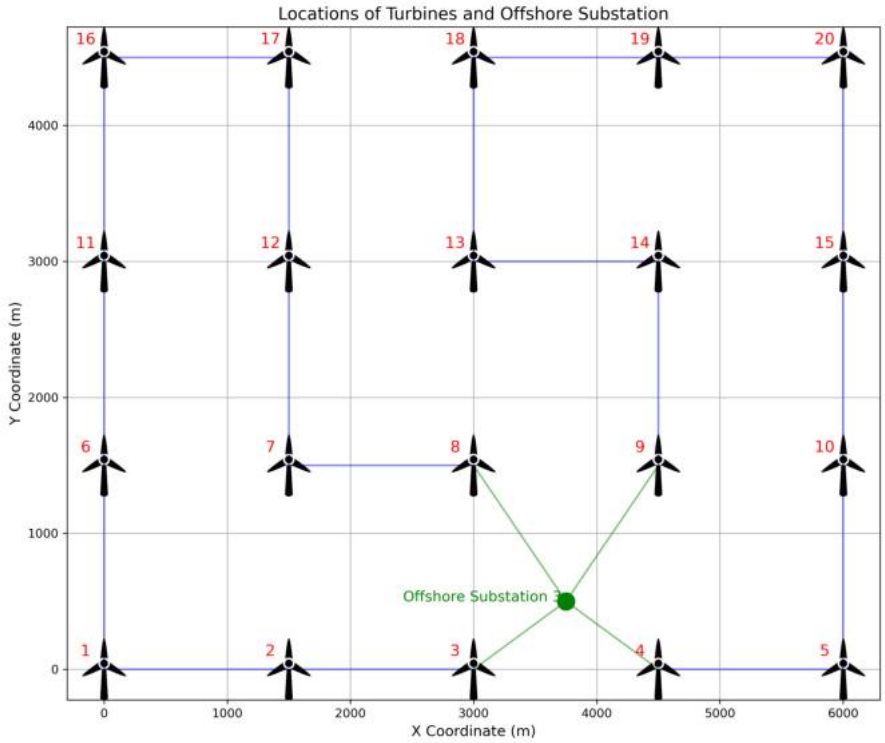

Figure 5.9: The Obtained Results Illustration for Ring Connection Configuration with Multiple Offshore Substation Candidate Locations

Table 5.15: The Obtained Optimal MV Cable Connection Between the Turbines for Ring Connection Configuration with Multiple Offshore Substation Candidate Locations

From	To	MV Cable Type
1	2	95 mm^2
2	3	95 mm^2
5	4	95 mm^2
6	1	95 mm^2
7	8	95 mm^2
10	5	95 mm^2
11	6	95 mm^2
12	7	95 mm^2
13	14	95 mm^2
14	9	95 mm^2
15	10	95 mm^2
16	11	95 mm^2
16	17	95 mm^2
17	12	95 mm^2
18	13	95 mm^2
19	18	95 mm^2
20	15	95 mm^2
20	19	95 mm^2

The connections between turbines and the selected offshore substation location (Location 3) are detailed in Table 5.16.

Table 5.16: The Obtained Optimal MV Cable Connection Between Turbines and Selected Offshore Substation for Ring Connection Configuration with Multiple Offshore Substation Candidate Locations

Turbine	MV Cable Type	Substation Location
3	150 mm^2	3
4	150 mm^2	3
8	150 mm^2	3
9	150 mm^2	3

The HVAC cable connecting the selected offshore substation to the PCC is summarized in Table 5.17, and its layout is illustrated in Figure 5.10.

Table 5.17: The Obtained Optimal HVAC Cable Connection Between Selected Offshore Substation and PCC for Ring Connection Configuration with Multiple Offshore Substation Candidate Locations with Multiple Offshore Substation Candidate Locations

HV Cable Type	Path	Substation Location
300 mm^2	1	3

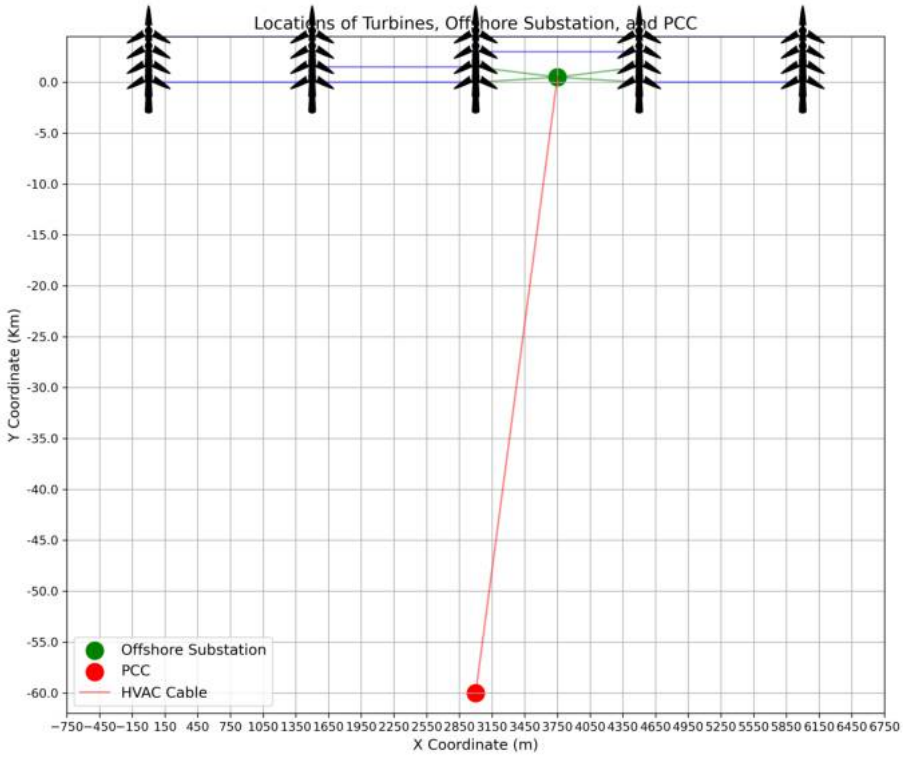

Figure 5.10: Illustration of HVAC Connection Between Selected Offshore Substation and PCC for Ring Connection Configuration with Multiple Offshore Substation Candidate Locations

The installed transformer in the selected offshore substation is summarized in Table 5.18.

Table 5.18: Installed Transformer Type and Position for Ring Connection Configuration with Multiple Offshore Substation Candidate Locations

Substation Location	Transformer Type	Transformer Position
3	200 MVA	1

The obtained costs, which include the total investment cost, total loss costs, wind curtailment cost, and total revenue, are detailed in Table 5.19.

Table 5.19: The Obtained Costs of Investment and Operation along with Revenue for Ring Connection Configuration with Multiple Offshore Substation Candidate Locations

Total Cost & Revenue Component	Value (K€)
Investment Cost	10,373.24
Loss Cost (HV Cables)	637.07
Loss Cost (HVDC Cables)	0
Loss Cost (HVDC VSC)	0
Wind Curtailment Cost	0
Revenue from Energy Sales	69,038.74
Operation Cost	637.07
Revenue - Cost	58,028.43

The total Revenue - Cost for this case with multiple offshore substation candidate locations is 58,028.43 K€, slightly more than the Revenue - Cost of 58,026.96 K€for the previous case with a fixed offshore substation. This difference, which is small in this case but can be significant in general, highlights the critical role of optimal offshore substation placement in minimizing costs and enhancing system efficiency. Strategic selection of the substation location can substantially reduce overall system costs while ensuring reliability and optimal operational performance.

5.3.3 Star Connection Configuration

The Star Connection Configuration is characterized by a direct connection between each turbine and the offshore substation, resulting in maximum reliability. In this design, a fault in any single cable impacts only the connected turbine, without affecting the operation of other turbines, which makes it highly fault-tolerant. However, this configuration comes at the cost of the highest investment due to the requirement for individual cables from each turbine to the offshore substation. The Star Connection Configuration is ideal for scenarios where ensuring maximum reliability and operational robustness is prioritized over cost minimization. The obtained results considering the constraints (4.55), (4.56), and the change in the α parameter of (4.51) (which is set to be equal to the total number of turbines), to guarantee a star connection configuration, are presented in this section.

5.3.3.1 Obtained Results Considering a Fixed Offshore Substation Location

The turbine locations and the fixed offshore substation location for the Star Connection Configuration are identical to those shown in Figure 5.3. The obtained results for the MV collection grid are illustrated in Figure 5.11, where all turbines are directly connected to the offshore substation without any inter-turbine connections to ensure star connection configuration. The details of the connections are summarized in Table 5.20.

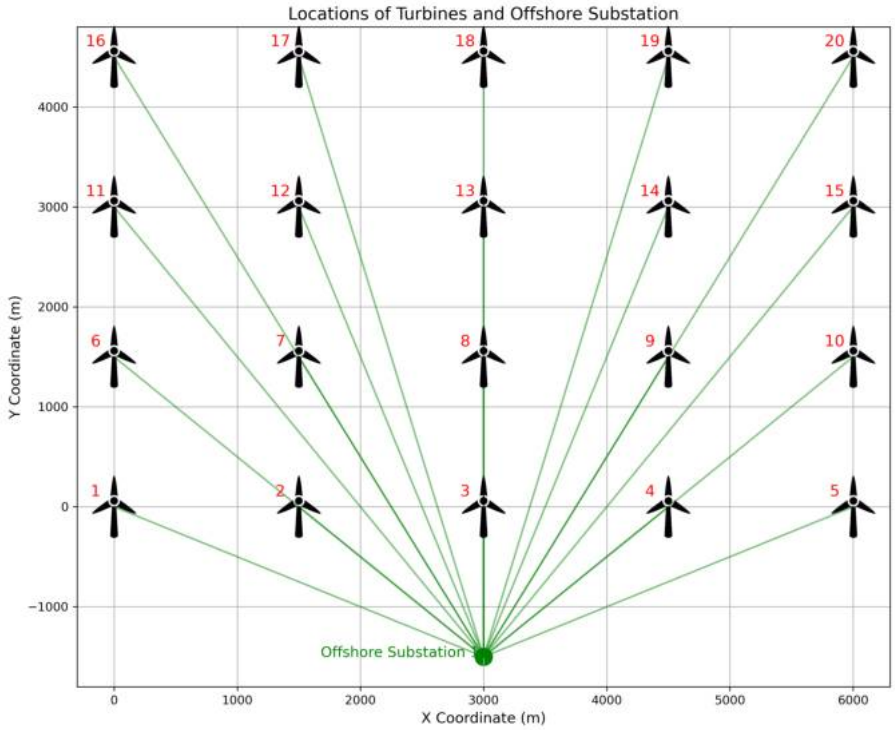

Figure 5.11: The Obtained Results Illustration for Star Connection Configuration with a Fixed Offshore Substation Location

Table 5.20: The Obtained Optimal MV Cable Connection Between Turbines and the Fixed Offshore Substation for Star Connection Configuration

Turbine	MV Cable Type
1	95 mm^2
2	95 mm^2
3	95 mm^2
4	95 mm^2
5	95 mm^2
6	95 mm^2
7	95 mm^2
8	95 mm^2
9	95 mm^2
10	95 mm^2
11	95 mm^2
12	95 mm^2
13	95 mm^2
14	95 mm^2
15	95 mm^2
16	95 mm^2
17	95 mm^2
18	95 mm^2
19	95 mm^2
20	95 mm^2

The installed HVAC cable connecting the offshore substation to the PCC is summarized in Table 5.21 and illustrated in Figure 5.12, also the installed transformer is detailed in Table 5.22.

Table 5.21: The Obtained Optimal HVAC Cable Connection Between the Fixed Offshore Substation and PCC for Star Connection Configuration

HV Cable Type	Path
300 mm^2	1

Table 5.22: Installed Transformer Type and Position in the Fixed Offshore Substation for Star Connection Configuration

Transformer Type	Position
200 MVA	1

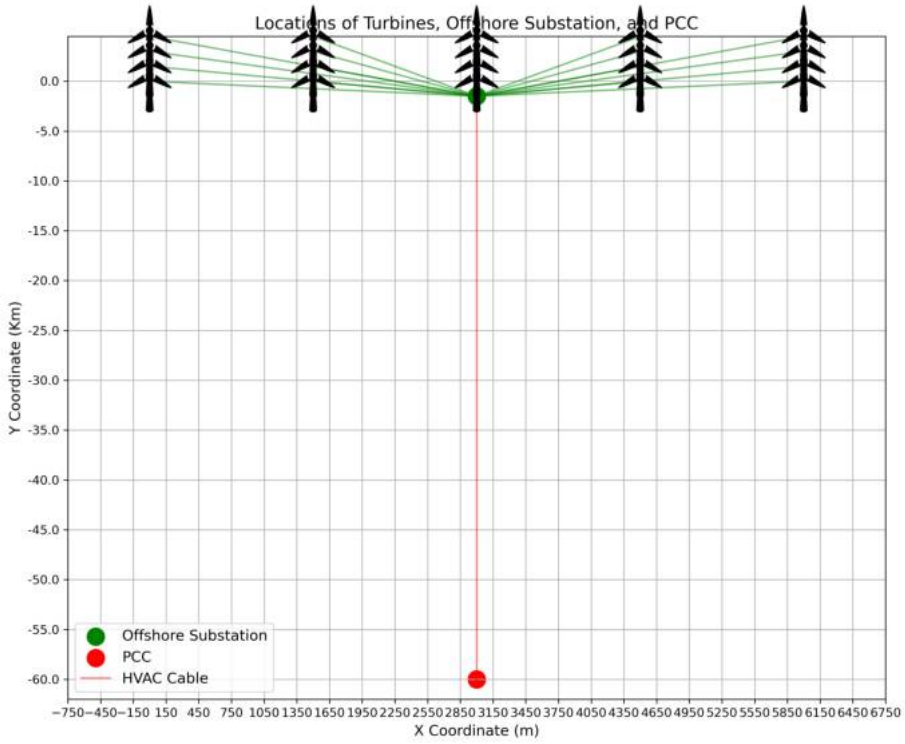

Figure 5.12: Illustration of HVAC Connection Between the Fixed Offshore Substation and PCC for Star Connection Configuration

The obtained costs and revenues for this case are detailed in Table 5.23.

The total Revenue - Cost for the Star Connection Configuration with a fixed offshore substation location is 56,067.91 K€, which is lower than both the Ring Connection Configuration (58,026.96 K€) and the Base Case (58,164.05 K€) with the same offshore substation location. While the Star Connection Configuration ensures maximum reliability by directly connecting each turbine to the offshore substation, it comes at the highest cost due to the cable requirements. In this configuration, a fault in a turbine-to-substation connection only impacts the

Table 5.23: The Obtained Costs of Investment and Operation for Star Connection Configuration with a Fixed Offshore Substation Location

Total Cost & Revenue Component	Value (K€)
Investment Cost	12,371.52
Loss Cost (HV Cables)	615.96
Loss Cost (HVDC Cables)	0
Loss Cost (HVDC VSC)	0.00
Wind Curtailment Cost	0
Revenue from Energy Sales	69,055.39
Operation Cost	615.96
Revenue - Cost	56,067.91

affected turbine, without disrupting the operation of other turbines. This makes the Star Connection highly fault-tolerant compared to the Ring and Radial Configuration. The trade-off between the Star Configuration's high reliability and its increased cost highlights its suitability for scenarios where operational robustness is prioritized.

5.3.3.2 Obtained Results Considering Multiple Candidate Offshore Substation Locations

The turbine positions and offshore substation candidate locations for this case are identical to those shown in Figure 5.7. The connection between turbines and the selected offshore substation (Location 3) is illustrated in Figure 5.13 and reported in Table 5.24.

Table 5.24: The Obtained Optimal MV Cable Connection Between Turbines and Selected Offshore Substation for Star Connection Configuration with Multiple Offshore Substation Candidate Locations

Turbine	MV Cable Type	Substation Location
1	95 mm^2	3
2	95 mm^2	3
3	95 mm^2	3
4	95 mm^2	3
5	95 mm^2	3
6	95 mm^2	3
7	95 mm^2	3
8	95 mm^2	3
9	95 mm^2	3
10	95 mm^2	3
11	95 mm^2	3
12	95 mm^2	3
13	95 mm^2	3
14	95 mm^2	3
15	95 mm^2	3
16	95 mm^2	3
17	95 mm^2	3
18	95 mm^2	3
19	95 mm^2	3
20	95 mm^2	3

The selected offshore substation is connected to the PCC using an HVAC cable, as summarized in Table 5.25, and its layout is illustrated in Figure 5.14.

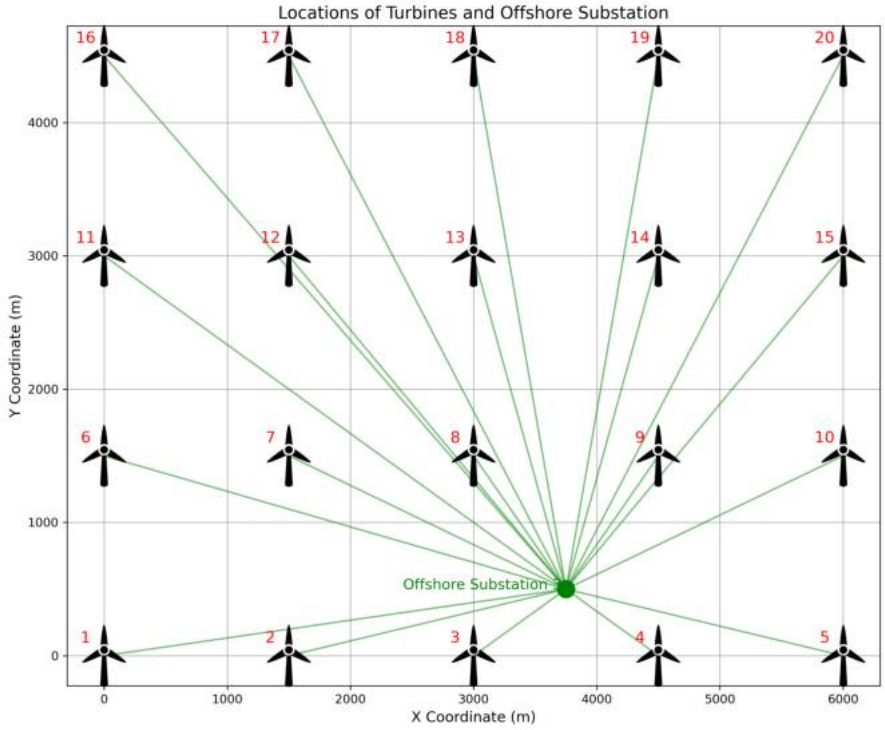

Figure 5.13: The Obtained Results Illustration for Star Connection Configuration with Multiple Offshore Substation Candidate Locations

Table 5.25: The Obtained Optimal HVAC Cable Connection Between Selected Offshore Substation and PCC for Star Connection Configuration with Multiple Offshore Substation Candidate Locations

HV Cable Type	Path	Substation Location
300 mm^2	1	3

The installed transformer in the selected offshore substation is detailed in Table 5.26.

Table 5.26: Installed Transformer Type and Position in Selected Offshore Substation for Star Connection Configuration with Multiple Offshore Substation Candidate Locations

Substation Location	Transformer Type	Transformer Position
3	200 MVA	1

The obtained costs and revenues for the Star Connection Configuration with multiple offshore substation candidate locations are detailed in Table 5.27.

The total Revenue - Cost for the Star Connection Configuration with multiple offshore substation candidate locations is 56,883.42 K€, which is higher than the Star Connection Configuration with a fixed offshore substation (56,067.91 K€). This demonstrates the importance of optimal offshore substation placement in reducing costs. By selecting the best substation location, overall system costs can be decreased while maintaining the maximum reliability provided by the Star Configuration.

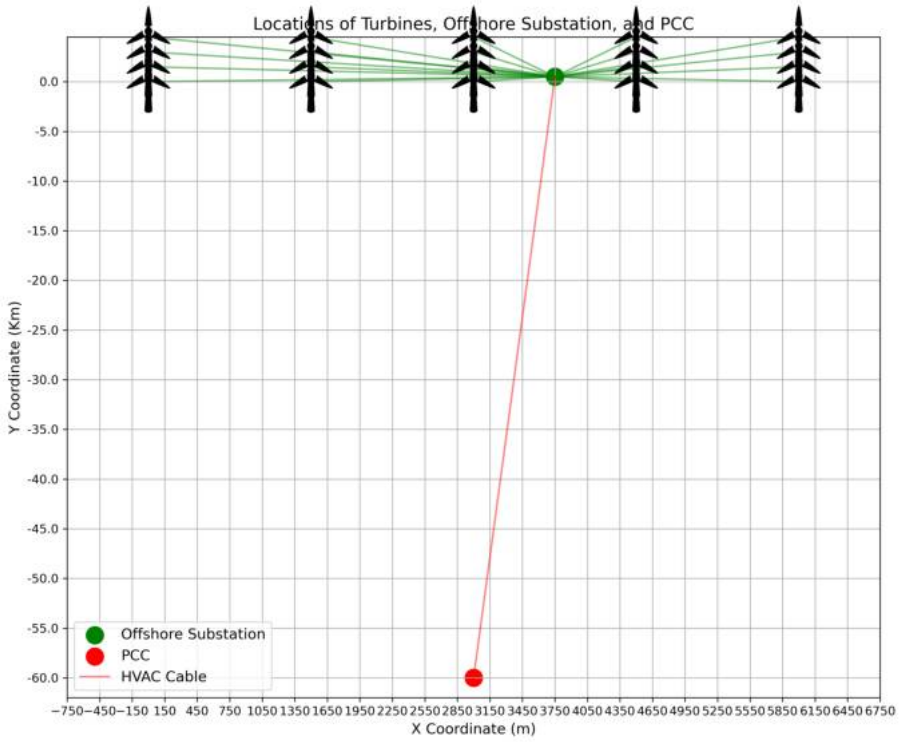

Figure 5.14: Illustration of HVAC Connection Between Selected Offshore Substation and PCC for Star Connection Configuration with Multiple Offshore Substation Candidate Locations

Table 5.27: The Obtained Costs of Investment and Operation for Star Connection Configuration with Multiple Offshore Substation Candidate Locations

Total Cost & Revenue Component	Value (K€)
Investment Cost	11,518.25
Loss Cost (HV Cables)	637.07
Loss Cost (HVDC Cables)	0
Loss Cost (HVDC VSC)	0.00
Wind Curtailment Cost	0
Revenue from Energy Sales	69,038.74
Operation Cost	637.07
Revenue - Cost	56,883.42

The total Revenue - Cost for the Star Connection Configuration with multiple offshore substation candidate locations is lower than both the Ring Connection Configuration (58,021.16 K€, Table 5.19) and the Base Case with Radial Configuration (58,164.05 K€, Table 5.9). While the Star Connection Configuration ensures maximum reliability by connecting each turbine directly to the offshore substation, it incurs higher costs due to the cable requirements. In contrast, the Ring and Radial Configurations achieve lower costs but offer reduced reliability. This comparison highlights the trade-off between cost and reliability, with the Star Configuration being suitable for scenarios prioritizing fault tolerance and robustness, while the Ring and Radial Configurations may be preferred for cost-sensitive applications.

5.3.4 HVDC Transmission Systems

High Voltage Direct Current (HVDC) transmission systems offer an efficient solution for transmitting power over long distances, making them ideal for remote offshore wind farms. Unlike HVAC systems, which face significant power losses and high costs over extended distances, HVDC systems reduce losses and improve transmission efficiency. By utilizing Voltage Source Converters (VSCs) and HVDC cables, these systems can ensure reliable and cost-effective power transfer, particularly for OWFs located far from the PCC. This section explores different scenarios to evaluate the performance and economic impact of HVAC and HVDC systems in remote OWFs.

5.3.4.1 Remote Offshore Wind Farm with HVAC Transmission System

In this case, the offshore wind farm is located remotely, with the PCC positioned 95,000 meters away from the first row of turbines. The connection to the PCC is achieved through transformers and long HVAC cables, without the possibility of using HVDC cables in this scenario.

The obtained results for the MV collection grid are identical to those reported in Table 5.5 and illustrated in Figure 5.4. Similarly, the MV cable connections between the turbines and the offshore substation remain the same as presented in Table 5.6.

The HVAC cable connecting the offshore substation to the PCC is summarized in Table 5.28, and the installed transformer is detailed in Table 5.29. The connection between the offshore substation and the PCC is illustrated in Figure 5.15.

Table 5.28: The Obtained Optimal HVAC Cable Connection Between Offshore Substation and PCC for Remote Offshore Wind Farm with HVAC Transmission System

HV Cable Type	Path
300 mm^2	1

Table 5.29: Installed Transformer Type and Position for Remote Offshore Wind Farm with HVAC Transmission System

Transformer Type	Position
200 MVA	1

The obtained costs and revenues for this scenario are detailed in Table 5.30.

The total Revenue - Cost for the remote OWF with HVAC transmission system is 53,868.37 K€. The higher losses and investment costs associated with long HVAC cables make this configuration less economically efficient, emphasizing the need to explore HVDC transmission systems for such remote OWFs.

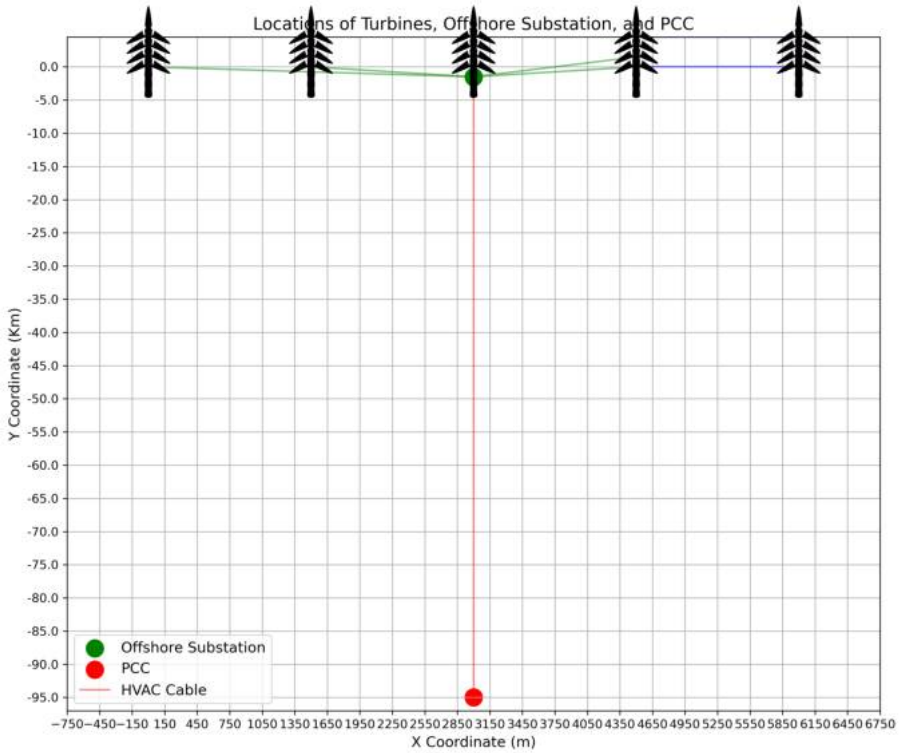

Figure 5.15: Illustration of Connection Between Offshore Substation and PCC for Remote Offshore Wind Farm with HVAC Transmission System

Table 5.30: The Obtained Costs of Investment and Operation for Remote Offshore Wind Farm with HVAC Transmission System

Total Cost & Revenue Component	Value (K€)
Investment Cost	13,911.78
Loss Cost (HV Cables)	984.48
Loss Cost (HVDC Cables)	0
Loss Cost (HVDC VSC)	0.00
Wind Curtailment Cost	0
Revenue from Energy Sales	68,764.63
Operation Cost	984.48
Revenue - Cost	53,868.37

The comparison between Figure 5.16 (remote OWF with HVAC transmission at 95 km) and Figure 5.6 highlights the impact of increased transmission distance on the transmitted power losses and consequently the delivered power to PCC.

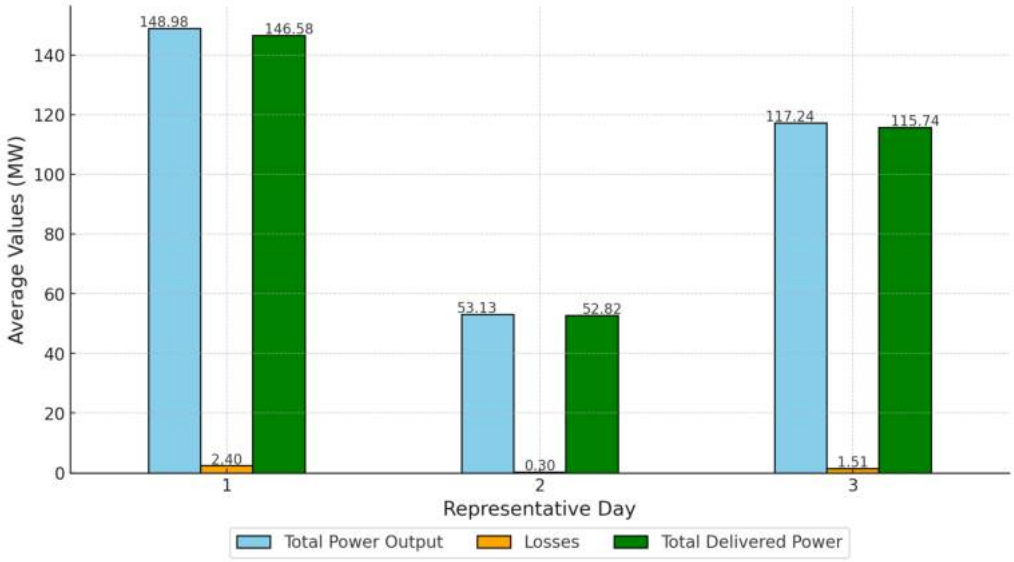

Figure 5.16: Illustration of Average Total Power Output, Losses, and Total Delivered Power per Representative Day for the Remote OWF with HVAC Transmission System

1. **Losses:** The power losses have increased in the remote OWF scenario due to the extended HVAC cable length. For instance, on Representative Day 1, the losses are approximately 1.50 MW in the base case (60 km) compared to 2.40 MW in the remote OWF (95 km). This trend is consistent across all representative days.

2. **Delivered Power to PCC:** The delivered power to the PCC has decreased slightly in the remote OWF case. On Representative Day 1, the delivered power in the base case is 147.48 MW, whereas, in the remote OWF, it is 146.58 MW. This reduction is primarily due to increased transmission losses over the longer distance.

As a conclusion, while HVAC transmission systems can handle longer distances, they incur significant losses and reduced efficiency, making HVDC transmission a more attractive solution for distances beyond 80 km [49].

5.3.4.2 Remote Offshore Wind Farm with HVDC Transmission System

This case considers a remote offshore wind farm located 95,000 meters from the PCC, similar to the previous scenario. However, in this case, HVDC transmission is allowed for connecting the offshore substation to the PCC. The results for the MV collection grid remain identical to the previous case and are detailed in Table 5.5 and Figure 5.4. The HVDC connection between the offshore substation and the PCC is illustrated in Figure 5.17, while the overall structure of the VSC-based HVDC system is depicted in Figure 5.18.

The installed HVDC cable, with a power capacity of 200 MW and a cross-sectional area of 240 mm^2, is summarized in Table 5.31. Additionally, VSCs with a capacity of 200 MW are installed at both ends of the HVDC transmission line.

The obtained costs and revenues for this scenario are summarized in Table 5.32.

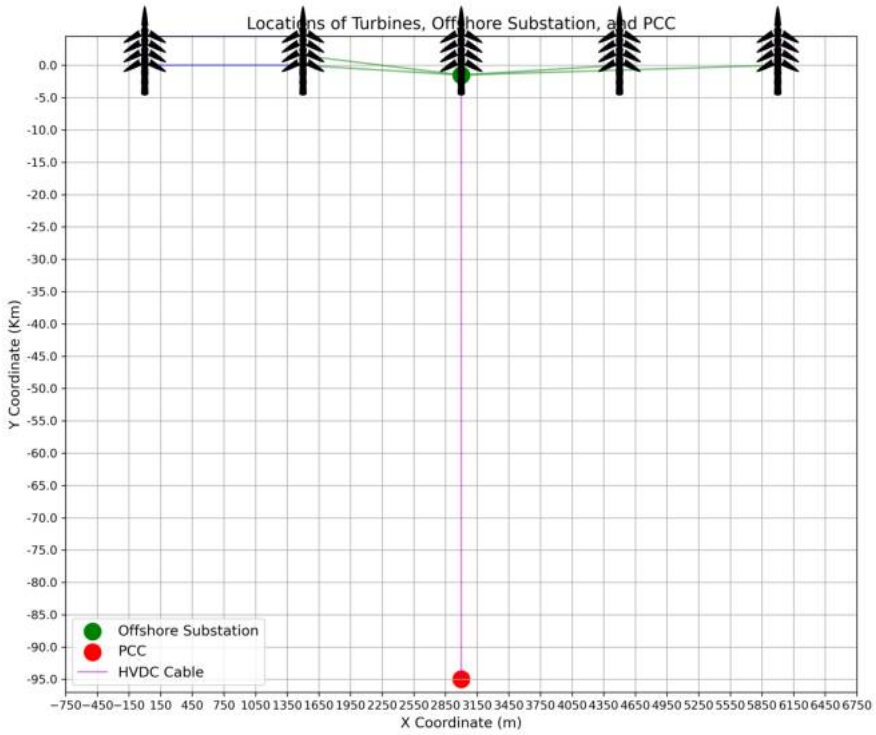

Figure 5.17: Illustration of HVDC Connection Between Offshore Substation and PCC for Remote OWF with HVDC Transmission System

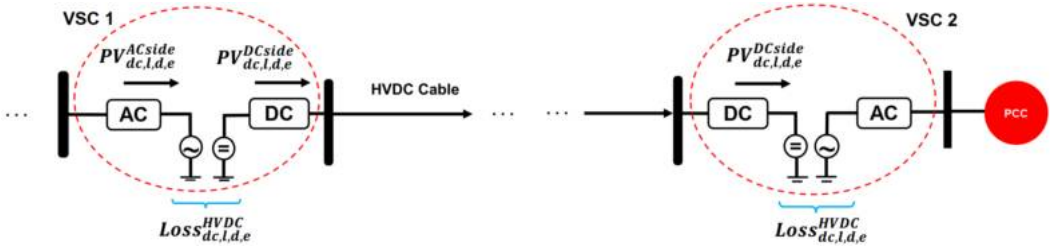

Figure 5.18: Overall Structure of the VSC-Based HVDC System for Remote OWF, Connecting Offshore Substation and PCC

Table 5.31: The Installed HVDC Cable for Remote Offshore Wind Farm with HVDC Transmission System

HVDC Cable Type
200 MW / 240 mm^2

Table 5.32: The Obtained Costs of Investment and Operation for Remote OWF with HVDC Transmission System

Total Cost & Revenue Component	Value (K€)
Investment Cost	12,940.21
Loss Cost (HV Cables)	0.00
Loss Cost (HVDC Cables)	123.87
Loss Cost (HVDC VSC)	486.26
Wind Curtailment Cost	0
Revenue from Energy Sales	69,027.07
Operation Cost	610.13
Revenue - Cost	55,476.73

The total Revenue - Cost for the remote OWF with HVDC transmission is 55,476.73 K€, which is higher than the HVAC transmission system case (53,868.37 K€). Despite the additional cost of VSCs, the HVDC system demonstrates a slightly lower overall investment cost compared to the HVAC system for a distance of 95 km. This is due to the higher efficiency of HVDC cables over long distances. Additionally, the reduced losses and improved operational efficiency of the HVDC system contribute to lower operational costs and increased economic performance, making it a more cost-effective solution for remote offshore wind farms.

This comparison demonstrates that for remote offshore wind farms, where the distance exceeds the breakeven point of approximately 80 km, HVDC transmission systems provide cost savings and efficiency improvements over HVAC systems.

5.3.5 Reliability Analyzing

This section evaluates the reliability of the three different collection grid configurations: Base Case (Radial), Ring, and Star configurations, each with a single fixed offshore substation location. To assess the impact of reliability, we consider a scenario where one of the MV cables connecting a turbine to the fixed offshore substation experiences a failure or outage. The analysis estimates the energy expected not served (EENS) or wind curtailment due to this failure, and the associated costs for each configuration.

In all three configurations, a cable failure is considered as the critical reliability event. The specific cable failure is assumed to occur on one of the MV cables directly connecting to the offshore substation. This outage prevents power transfer from the connected turbine(s) to the substation, resulting in wind energy curtailment.

To account for real-world conditions, we assume two failures per year, each resulting in 20 days of interruption. This equates to a total interruption time of:

$$\text{Total Interruption Time per Year} = 2 \times 20 \times 24 = \textbf{960 hours/year}.$$

The amount of curtailed energy and the associated costs are calculated based on the configuration's design and the total interruption hours.

5.3.5.1 Reliability Analysis for Base Case (Radial Configuration)

In the Base Case with a radial collection grid, the failure of a single cable affects not only the turbine connected to the failed cable but also the entire branch of turbines downstream of the

failure, as illustrated in Figure 5.19. This cascading impact results in significant wind energy curtailment, as the power from the affected turbines cannot be transmitted to the offshore substation.

The total wind curtailment cost for the radial configuration is calculated to be 1,763.44 K€for 960 hours of interruption per year. This significant cost highlights the vulnerability of radial configurations to single-point failures which emphasizes the importance of more resilient designs for offshore wind farm collection grids.

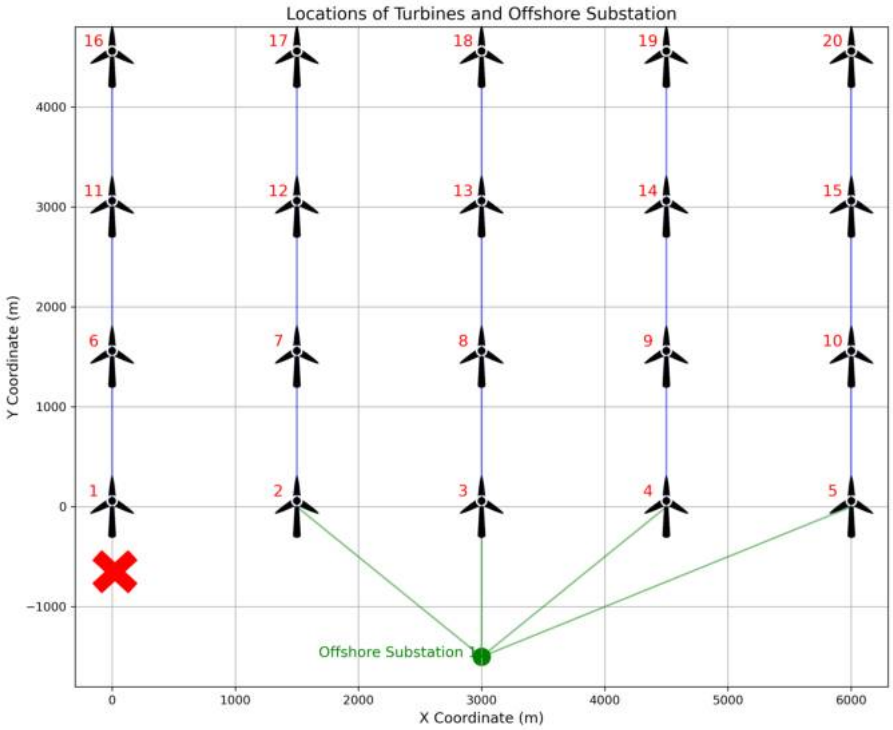

Figure 5.19: Impact of a Single Cable Failure in a Radial Collection Grid Configuration

Table 5.33: Wind Curtailment Cost for Radial Configuration Under Single Cable Failure Considering the Total Interruption Time per Year

Parameter	Value (K€/ year)
Total Wind Curtailment Cost	**1,763.44**

5.3.5.2 Reliability Analysis for Ring Configuration

In the Ring Configuration, each turbine is connected through two paths, providing redundancy. When a single cable fails, as illustrated in Figure 5.20, the redundancy ensures that the power from the affected turbine(s) can still be transmitted through the alternative path. This design mitigates the impact of a single cable failure, resulting in lower wind energy curtailment compared to the radial configuration.

The total wind curtailment cost for the Ring Configuration is calculated to be 1,227.52 K€for 960 hours of interruption per year. This reduction in wind curtailment cost highlights the improved

reliability and fault tolerance of the Ring Configuration.

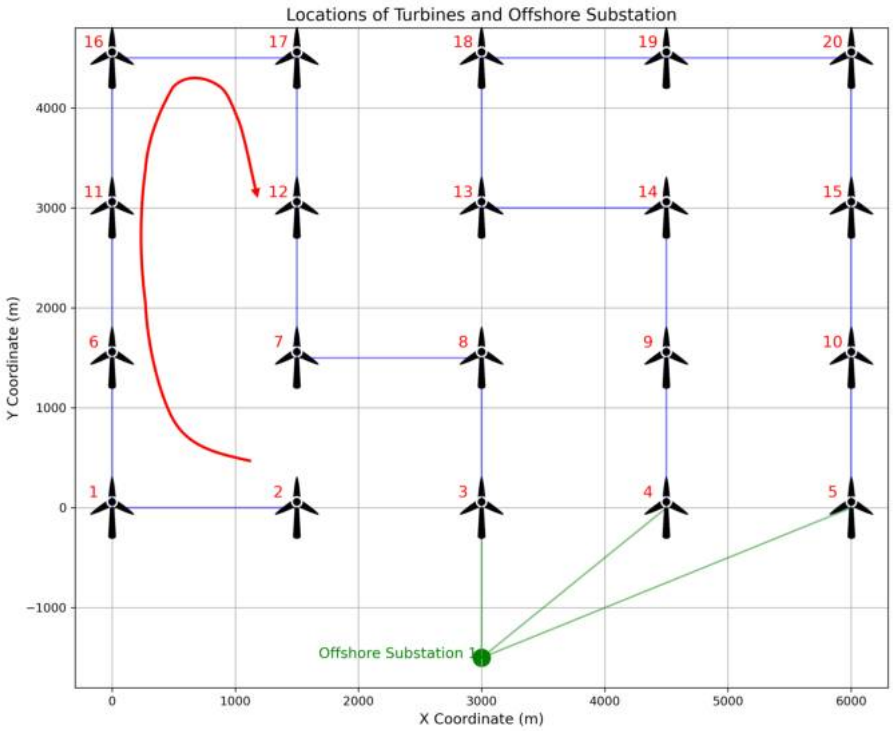

Figure 5.20: Impact of a Single Cable Failure in a Ring Collection Grid Configuration

Table 5.34: Wind Curtailment Cost for Ring Configuration Under Single Cable Failure Considering the Total Interruption Time per Year

Parameter	Value (K€/year)
Total Wind Curtailment Cost	**1,227.52**

Compared to the Base Case (Radial Configuration), which has a total wind curtailment cost of 1,763.44 K€, the Ring Configuration reduces the wind curtailment cost by approximately **30.4%**. This demonstrates the substantial reliability benefits of introducing redundancy into the collection grid, which translates into significant cost savings over the lifetime of the system.

5.3.5.3 Reliability Analysis for Star Configuration

In the Star Configuration, each turbine is directly connected to the offshore substation with its own dedicated cable. A cable failure only impacts the turbine connected to the failed cable, and no other turbines are affected. This design isolates failures and minimizes their impact, ensuring that the overall wind energy curtailment remains significantly lower compared to the Radial and Ring Configurations.

The EENS for this configuration is determined solely by the power output of the single affected turbine during the total interruption time. The total wind curtailment cost for the Star Configuration is calculated to be 440.86 K€for 960 hours of interruption per year, as shown in Table 5.35. This highlights the advantage of the Star Configuration in minimizing the impact of cable

failures on system reliability, as each turbine operates independently with no cascading effects from single cable outages.

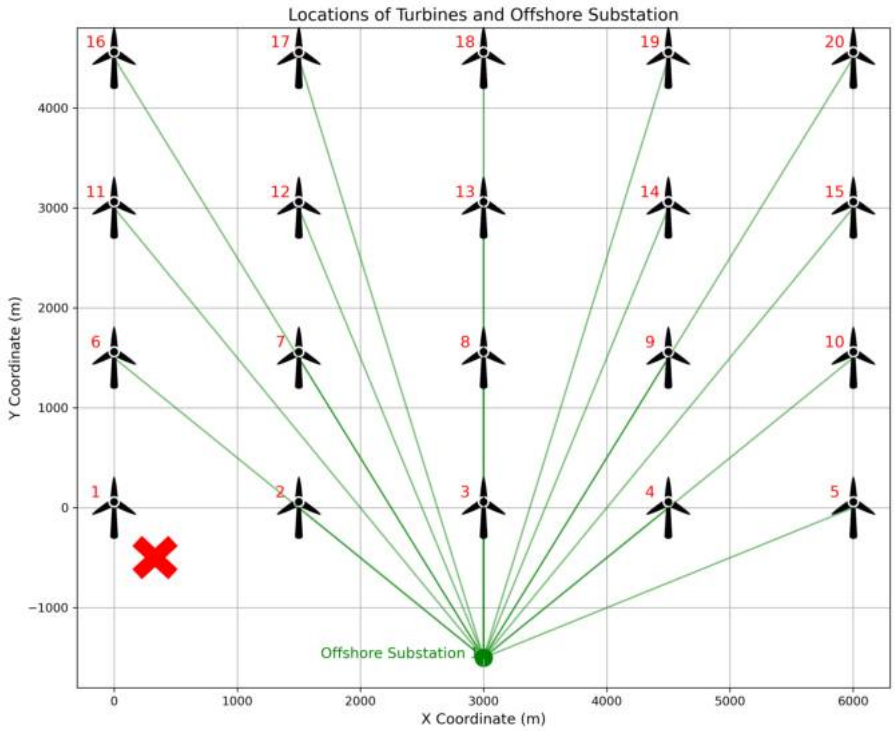

Figure 5.21: Impact of a Single Cable Failure in a Star Collection Grid Configuration

Table 5.35: Wind Curtailment Cost for Star Configuration Under Single Cable Failure Considering the Total Interruption Time per Year

Parameter	Value (K€/year)
Total Wind Curtailment Cost	**440.86**

Compared to the Base Case (Radial Configuration) with a total wind curtailment cost of 1,763.44 K€and the Ring Configuration with a cost of 1,227.52 K€, the Star Configuration achieves a substantial reduction in wind curtailment costs by **75.0%** and **64.1%**, respectively. This highlights the Star Configuration's superior fault isolation capability, effectively minimizing energy losses during cable outages.

Table 5.36 highlights the total wind curtailment costs per year for different collection grid configurations under a single cable failure scenario. The results demonstrate that the Star Configuration significantly reduces curtailment costs due to its superior fault isolation, while the Ring Configuration offers moderate reductions through redundancy compared to the Radial (Base Case).

Table 5.36: Comparison of Wind Curtailment Costs and Reductions for Different Configurations

Configuration	Wind Curtailment Cost (K€)	Reduction Compared to Radial (%)	Reduction Compared to Ring (%)
Radial (Base Case)	1763.44	0	-
Ring	1227.52	**30.4**	0
Star	440.86	**75**	**64.1**

5.4 Results Comparison

In this section, the obtained results are compared to provide insights into the cost efficiency of each connection configuration between the turbines.

The comparison of Revenue - Cost (K€) for the Radial (Base Case), Ring, and Star configurations is shown in Figure 5.22. This comparison highlights the differences in economic performance among the configurations when considering a fixed offshore substation.

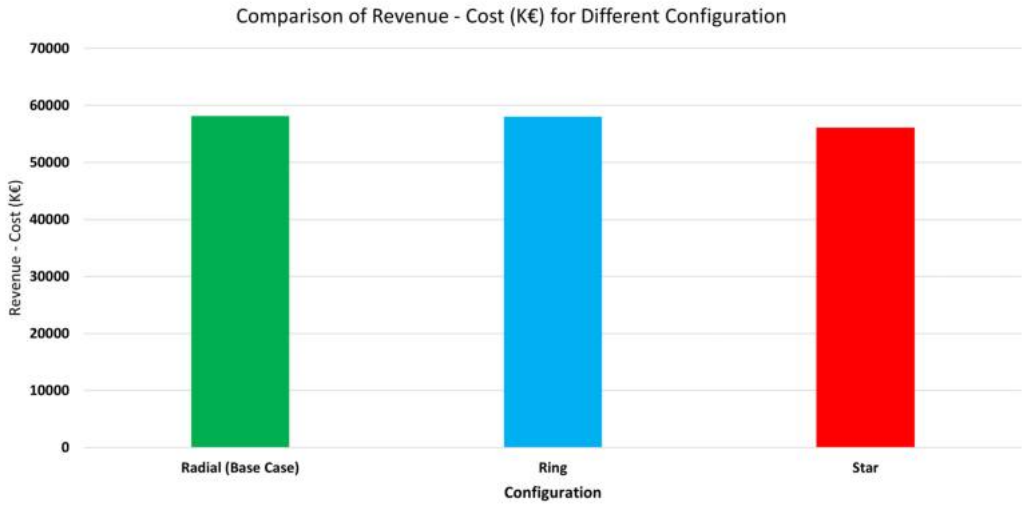

Figure 5.22: Comparison of Revenue - Cost (K€) for Different Configurations with a Fixed Offshore Substation

As presented in Figure 5.22, the Revenue - Cost values for the three configurations are derived from the following tables: *Radial (Base Case) configuration*: Revenue - Cost of 58,164.05 K€, based on Table 5.9. *Ring Configuration*: Revenue - Cost of 58,026.96 K€, based on Table 5.14. *Star Configuration*: Revenue - Cost of 56,067.91 K€, based on Table 5.23.

The Radial (Base Case) configuration demonstrates the highest Revenue - Cost value, followed by the Ring Configuration, with the Star Configuration showing the lowest value. This highlights the trade-off between cost efficiency and system reliability among the configurations.

To provide a clearer view of the differences between the configurations, a zoomed-in version of the chart is presented in Figure 5.23.

Figure 5.23 emphasizes the marginal differences between the Radial and Ring configurations.

Figures 5.24 and 5.25 compare the Revenue - Cost outcomes for Radial, Ring, and Star configurations under fixed and multiple offshore substation scenarios. The results highlight that multiple substation locations can slightly improve economic performance, particularly for the Ring and Star configurations.

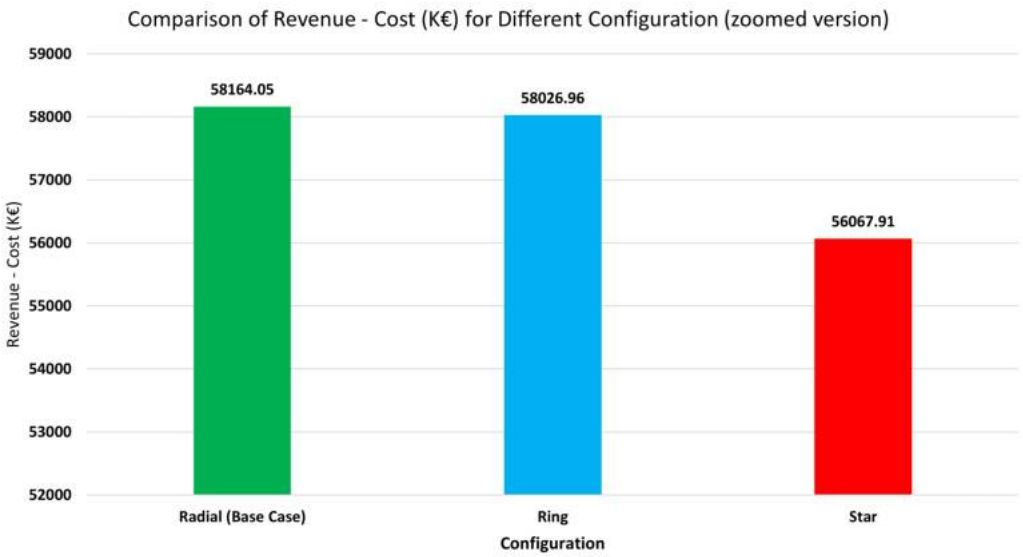

Figure 5.23: Comparison of Revenue - Cost (K€) for Different Configurations (Zoomed-In View)

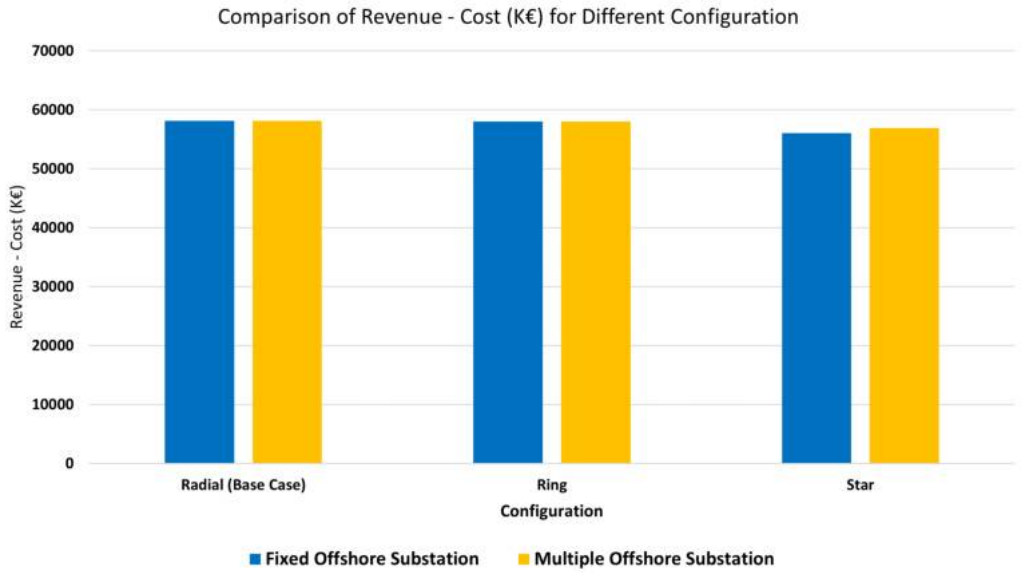

Figure 5.24: Comparison of Revenue - Cost (K€) for Different Configurations with Fixed and Multiple Offshore Substation Locations

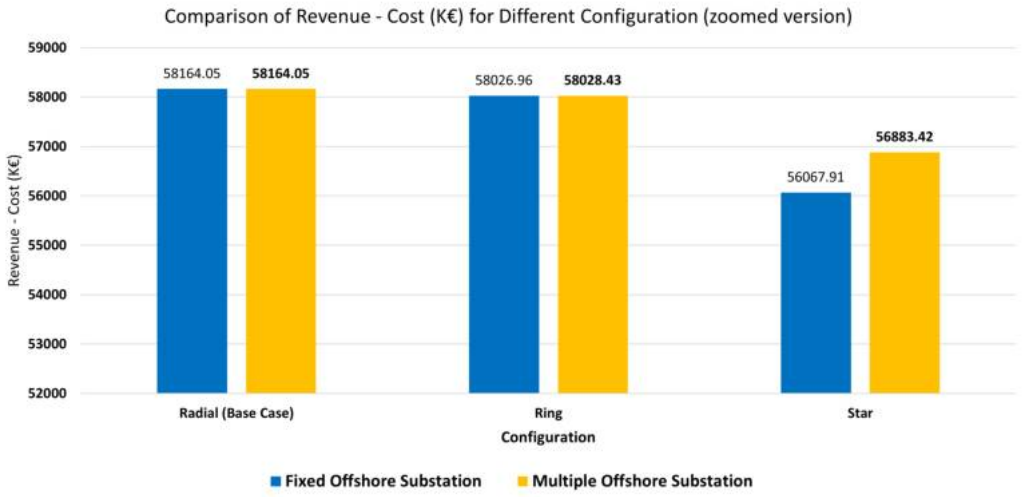

Figure 5.25: Zoomed Comparison of Revenue - Cost (K€) for Different Configurations with Fixed and Multiple Offshore Substation Locations

The figures in 5.26 and its zoomed version 5.27 illustrate the comparison of Revenue - Cost values for a remote offshore wind farm with two transmission system configurations: HVAC and HVDC. These comparisons highlight the economic superiority of the HVDC system for remote offshore wind farms.

As depicted in the charts, the HVDC system achieves a higher Revenue - Cost value of 55,476.73 K€, compared to the HVAC system's 53,868.37 K€. The zoomed version emphasizes this difference more clearly, demonstrating the improved cost efficiency of the HVDC configuration. This economic advantage is attributed to reduced energy losses and enhanced performance over long-distance energy transmission, as supported by the results presented in Table 5.30 and Table 5.32.

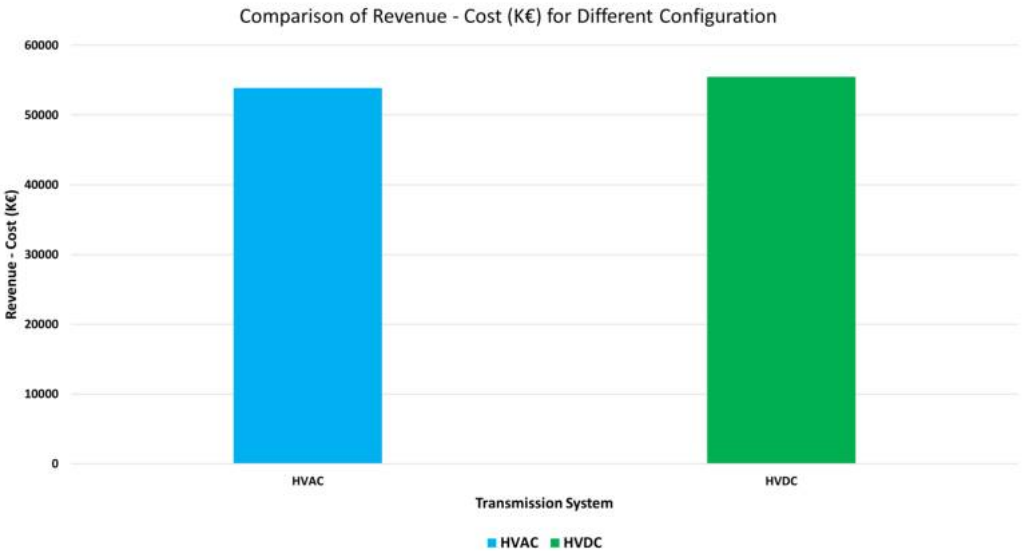

Figure 5.26: Comparison of Revenue - Cost (K€) for a Remote Offshore Wind Farm with HVAC and HVDC Transmission Systems

Figure 5.28 illustrates the comparison of wind energy curtailment costs and reductions for

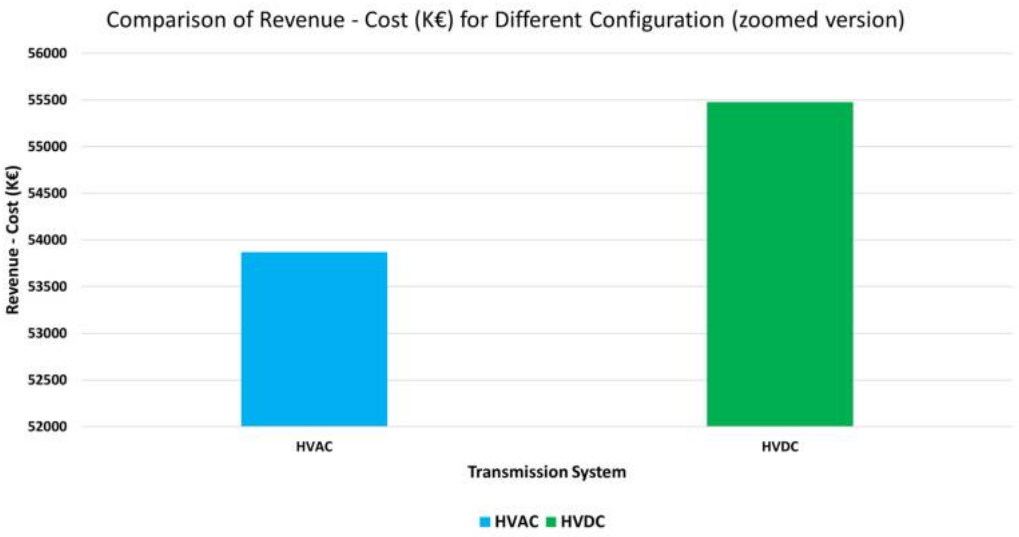

Figure 5.27: Comparison of Revenue - Cost (K€) for a Remote Offshore Wind Farm with HVAC and HVDC Transmission Systems (Zoomed Version)

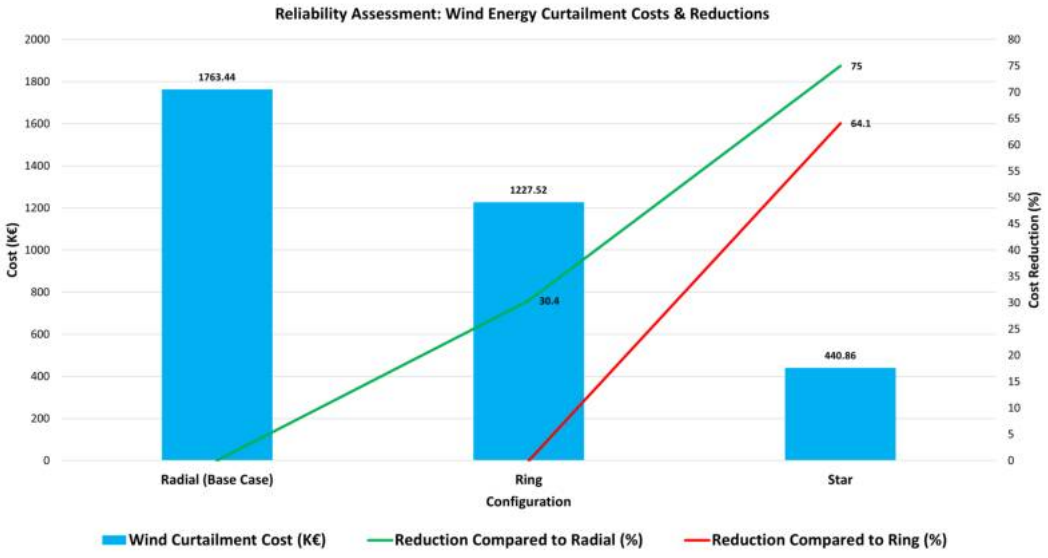

Figure 5.28: Reliability Assessment: Wind Energy Curtailment Costs and Reductions for Different Configurations

three different configurations: Radial (Base Case), Ring, and Star. The blue bars represent the wind curtailment costs in K€, while the green and red lines show the percentage reductions compared to the Radial and Ring configurations, respectively.

The Star configuration demonstrates the highest reliability with a wind curtailment cost of 440.86 K€, achieving a 75% reduction compared to the Radial configuration and a 64.1% reduction compared to the Ring configuration. This highlights the superior fault isolation and minimal energy loss achieved with the Star configuration, as opposed to the higher curtailment costs observed in the Radial and Ring configurations.

6 Conclusions and Future Directions

6.1 Conclusions

This research project establishes a robust framework aimed at enhancing the efficiency, reliability, and cost-effectiveness of offshore wind farm (OWF) collection grids. By employing advanced optimization techniques, the study holistically addresses key elements of OWF design, including substation placement, connection configurations, and hybrid HVAC/HVDC transmission system selection. Through detailed modeling and analysis, it delivers actionable insights to boost the economic performance and operational stability of offshore wind energy systems.

An important achievement of this project is the development and application of a Mixed-Integer Linear Programming (MILP) optimization model. This model integrates crucial datasets, such as historical wind patterns, turbine power curves, cable characteristics, and energy market price forecasts, to minimize total costs while maximizing revenue. Its adaptability across various scenarios, especially those involving multiple offshore substation placement options and remote offshore wind farm locations, underscores its effectiveness as a decision-support tool for OWF planning and operations.

The comparative analysis of radial, ring, and star connection configurations reveals trade-offs among cost, reliability, and energy curtailment. The radial configuration is the most cost-efficient under standard conditions but is highly susceptible to cable failures, leading to considerable energy curtailment. The ring configuration, offering redundant pathways, improves reliability with a modest cost increase. Conversely, the star configuration, despite its higher initial cost, proves to be the optimal solution for minimizing energy curtailment during probable cable outages. These findings bring out the importance of tailoring grid configurations to the specific technical and economic needs of each offshore wind farm.

Furthermore, the study highlights the importance of offshore substation location optimization. Through a comparison of fixed substation placements with scenarios involving multiple candidate locations, the research shows that strategic substation placement improves financial performance. Optimizing substation locations reduces costs and boosts net revenue, underscoring its essential role in enhancing the economic viability of offshore wind farms.

Additionally, the research evaluates HVAC and HVDC transmission systems for remote offshore wind farms. The findings demonstrate that HVDC systems, with reduced energy losses and superior performance over long distances, offer higher cost efficiency. This reinforces the value of advanced transmission technologies in meeting the challenges of remote, large-scale offshore wind farms.

In conclusion, this research lays a foundation for the design and optimization of offshore wind energy systems. By addressing current challenges and aligning with the global transition to renewable energy, it supports the development of sustainable, reliable power grids to meet both present and future energy demands.

6.2 Future Directions

While this research provides meaningful contributions, there are several directions for further exploration:

1. **Integration of Hybrid Transmission Systems:** Investigate the potential of combining HVAC and HVDC systems to leverage their complementary strengths. Hybrid systems may offer versatile solutions for mid-range distances and intricate grid layouts.
2. **Incorporation of Energy Storage:** Explore the use of energy storage technologies, such as batteries or hydrogen-based solutions, to enhance grid reliability and manage power generation fluctuations. This could enable more efficient energy utilization and reduced curtailment.
3. **Advanced Reliability Assessments:** Expand reliability studies to consider multi-failure scenarios, extreme weather impacts, and aging infrastructure. This would provide a deeper understanding of grid resilience.
4. **Dynamic Thermal Rating for Cable Utilization:** Investigate the use of dynamic thermal rating (DTR) methods to optimize the utilization of submarine cables. By accounting for real-time thermal loading conditions, DTR can enable higher current-carrying capacity, reduce losses, and extend cable lifespan, improving the overall efficiency of offshore grid systems.
5. **Economic Feasibility of Emerging Technologies:** Examine the cost-effectiveness of cutting-edge technologies, such as superconducting cables and modular HVDC systems, for offshore wind farm applications.
6. **Scalability for Large-Scale Offshore Energy Systems:** Extend the optimization framework to include future multi-terminal offshore grids and energy hubs, integrating multiple renewable sources like solar and wave energy. In this project, due to the lack of access to efficient solvers such as Gurobi, we could not address higher levels of complexity in the optimization process. Future work should explore the use of advanced solvers or heuristic-based methods to handle the computational demands of more complex scenarios.

By pursuing these future directions, offshore wind energy systems can become more efficient, resilient, and sustainable, contributing to a carbon-neutral energy future. Continued research and innovation in this field are crucial for achieving global renewable energy goals.

6.3 Code Availability

The source code for this project, **OWFOptimizer**, is publicly available on GitLab. It can be accessed at the following URL:

`https://gitlab.tsn.tno.nl/moradisepahvandm/OWFOptimizer`

References

[1] Bo Yang et al. “A critical survey of technologies of large offshore wind farm integration: Summary, advances, and perspectives”. In: *Protection and Control of Modern Power Systems* 7.2 (2022), pp. 1–3.

[2] Shenquan Liu et al. “Integrating offshore wind power via fractional frequency transmission system”. In: *IEEE Transactions on Power Delivery* 32.3 (2015), pp. 1253–1261.

[3] Syed Wajahat Ali et al. “Offshore wind farm-grid integration: A review on infrastructure, challenges, and grid solutions”. In: *Ieee Access* 9 (2021), pp. 102811–102827.

[4] Rehana Perveen, Nand Kishor, and Soumya R Mohanty. “Off-shore wind farm development: Present status and challenges”. In: *Renewable and Sustainable Energy Reviews* 29 (2014), pp. 780–792.

[5] Abdulrahman Alassi et al. “HVDC transmission: Technology review, market trends and future outlook”. In: *Renewable and Sustainable Energy Reviews* 112 (2019), pp. 530–554.

[6] Hongyu Zhou et al. “Coordinated power control of electrochemical energy storage for mitigating subsequent commutation failures of HVDC”. In: *International Journal of Electrical Power & Energy Systems* 134 (2022), p. 107455.

[7] Ashkan Nami et al. “Control of the parallel operation of DR-HVDC and VSC-HVDC for offshore wind power transmission”. In: *IEEE Transactions on Power Delivery* 37.3 (2021), pp. 1682–1691.

[8] Nathalie Holtsmark et al. “An all-DC offshore wind farm with series-connected turbines: An alternative to the classical parallel AC model?” In: *IEEE Transactions on industrial Electronics* 60.6 (2012), pp. 2420–2428.

[9] Christoffer Fjellstedt et al. “A review of ac and dc collection grids for offshore renewable energy with a qualitative evaluation for marine energy resources”. In: *Energies* 15.16 (2022), p. 5816.

[10] Padmavathi Lakshmanan, Ruijuan Sun, and Jun Liang. “Electrical collection systems for offshore wind farms: A review”. In: *CSEE Journal of Power and Energy Systems* 7.5 (2021), pp. 1078–1092.

[11] H Hunter et al. “A study of submarine power grid planning for offshore wind farm”. In: *Proc. IEEE Power Energy Soc. Gen. Meet.* 2011, pp. 1–5.

[12] A Madariaga et al. “Technological trends in electric topologies for offshore wind power plants”. In: *Renewable and Sustainable Energy Reviews* 24 (2013), pp. 32–44.

[13] Jens Nørkær Sørensen and Gunner Christian Larsen. “A minimalistic prediction model to determine energy production and costs of offshore wind farms”. In: *Energies* 14.2 (2021), p. 448.

[14] Adam J Collin et al. “Electrical components for marine renewable energy arrays: A techno-economic review”. In: *Energies* 10.12 (2017), p. 1973.

[15] *Siemens Energy Subsea Transformers*. URL: `https://www.siemens-energy.com/global/en/offerings/industrialapplications/oil-gas/subsea-solutions/subsea-transformers.html` (visited on 04/25/2024).

[16] *Hitachi Energy Subsea Transformers*. URL: `https://www.hitachienergy.com/offering/product-and-system/transformers/special-application-transformers/subsea-transformers` (visited on 04/25/2024).

[17] Kabeya Musasa et al. “Review on DC collection grids for offshore wind farms with high-voltage DC transmission system”. In: *IET Power Electronics* 10.15 (2017), pp. 2104–2115.

[18] Yang Fu et al. “Collection system topology for deep-sea offshore wind farms considering wind characteristics”. In: *IEEE Transactions on Energy Conversion* 37.1 (2021), pp. 631–642.

[19] Feng An et al. “Multi-functional DC collector for future ALL-DC offshore wind power system: Concept, scheme, and implement”. In: *IEEE Transactions on Industrial Electronics* 69.8 (2021), pp. 8134–8145.

[20] Sara Lumbreras and Andres Ramos. “Optimal design of the electrical layout of an offshore wind farm applying decomposition strategies”. In: *IEEE Transactions on Power Systems* 28.2 (2012), pp. 1434–1441.

[21] Adelaide Cerveira et al. “Optimal cable design of wind farms: The infrastructure and losses cost minimization case”. In: *IEEE Transactions on Power Systems* 31.6 (2016), pp. 4319–4329.

[22] Tengjun Zuo et al. “A two-layer hybrid optimization approach for large-scale offshore wind farm collector system planning”. In: *IEEE Transactions on Industrial Informatics* 17.11 (2021), pp. 7433–7444.

[23] Gayan Abeynayake et al. “Analytical model for availability assessment of large-scale offshore wind farms including their collector system”. In: *IEEE Transactions on Sustainable Energy* 12.4 (2021), pp. 1974–1983.

[24] Tengjun Zuo et al. “Collector system topology design for offshore wind farm’s repowering and expansion”. In: *IEEE Transactions on Sustainable Energy* 12.2 (2020), pp. 847–859.

[25] Abdulrahman Alassi et al. “HVDC Transmission: Technology Review, Market Trends and Future Outlook”. In: *Renewable and Sustainable Energy Reviews* 112 (2019), pp. 530–554.

[26] *Engineering LibreTexts 2.2: Transmission Line Theory*. URL: `https://eng.libretexts.org/Bookshelves/Electrical_Engineering/Electronics/Book%3A_Semiconductor_Devices_Theory_and_Application_(Casell)/02%3A_Transmission_Lines/2.02%3A_Transmission_Line_Theory` (visited on 04/25/2023).

[27] Tarek Abedin et al. “Dynamic modeling of hvdc for power system stability assessment: A review, issues, and recommendations”. In: *Energies* 14.16 (2021), p. 4829.

[28] Xian Liu. “An Improved Interpolation Method for Wind Power Curves”. In: *IEEE Transactions on Sustainable Energy* 3.3 (2012), pp. 528–534. DOI: 10.1109/TSTE.2012.2191582.

[29] Frank Nielsen. “Hierarchical Clustering”. In: *Introduction to HPC with MPI for Data Science*. Cham: Springer International Publishing, 2016, pp. 195–211. ISBN: 978-3-319-21903-5. DOI: 10.1007/978-3-319-21903-5_8. URL: `https://doi.org/10.1007/978-3-319-21903-5_8`.

[30] RVO. *Permits for wind farms at IJmuiden Ver Gamma-A and Gamma-B, and Nederwiek I-A*. `https://www.rvo.nl/onderwerpen/windenergie-op-zee/ijmuiden-ver-gamma-nederwiek-i`. Accessed: 10.12.2024.

[31] Ke Meng et al. “Offshore transmission network planning for wind integration considering AC and DC transmission options”. In: *IEEE Transactions on Power Systems* 34.6 (2019), pp. 4258–4268.

[32] Wang Feng et al. “A new approach for benefit evaluation of multiterminal VSC–HVDC using a proposed mixed AC/DC optimal power flow”. In: *IEEE Transactions on Power Delivery* 29.1 (2013), pp. 432–443.

[33] Jean-Baptiste Hiriart-Urruty and Claude Lemaréchal. “Convex Analysis and Minimization Algorithms I: Fundamentals”. In: *Springer* (1993), pp. 10–15. DOI: 10.1007/978-3-642-85068-5.

[34] Tengjun Zuo et al. “Offshore wind farm collector system layout optimization based on self-tracking minimum spanning tree”. In: *International Transactions on Electrical Energy Systems* 29.2 (2019), e2729.

[35] Ahmed Reda et al. “Guidelines for safe cable crossing over a pipeline”. In: *Applied Ocean Research* 102 (2020), p. 102284.

[36] Arne Klein and Dag Haugland. “Obstacle-aware optimization of offshore wind farm cable layouts”. In: *Annals of Operations Research* 272.1 (2019), pp. 373–388.

[37] ABB. *XLPE Submarine Cable Systems: Attachment to XLPE Land Cable Systems*. Accessed: 2025-01-05. 2010. URL: https://new.abb.com/docs/default-source/ewea-doc/xlpe-submarine-cable-systems-2gm5007.pdf.

[38] J. Smith and A. Doe. “Cost Analysis of AC Cable Systems for Offshore Wind Power Transmission”. In: *IEEE Transactions on Power Delivery* (2019). Accessed: 2025-01-05. URL: https://ieeexplore.ieee.org/abstract/document/8878128.

[39] Danish Energy Agency. *Technology Data Catalogue for Electricity and District Heating*. Accessed: 2025-01-05. 2020. URL: https://ens.dk/sites/ens.dk/files/Analyser/technology_data_catalogue_for_el_and_dh.pdf.

[40] Danish Energy Agency. *Technology Catalogue Offshore Wind - Annex to Performance and Cost Predictions*. Accessed: 2025-01-05. 2022. URL: https://ens.dk/sites/ens.dk/files/Statistik/technology_catalogue_offshore_wind_march_2022_-_annex_to_prediction_of_performance_and_cost.pdf.

[41] ENTSO-E. *European Offshore Grid – Offshore Technology*. Accessed: 2025-01-05. 2020. URL: https://www.entsoe.eu/fileadmin/user_upload/_library/publications/entsoe/SDC/European_offshore_grid_-_Offshore_Technology_-_FINALversion.pdf.

[42] Netzentwicklungsplan. *Netzentwicklungsplan 2035, Version 2021, Part 2*. Accessed: 2025-01-05. 2021. URL: https://www.netzentwicklungsplan.de/sites/default/files/paragraphs-files/NEP_2035_V2021_2_Entwurf_Teil1.pdf.

[43] e-CIGRE. *Guidelines for the Design and Construction of AC Offshore Substations for Wind Power Plants*. Accessed: 2025-01-05. 2021. URL: https://www.e-cigre.org/publications/detail/483-guidelines-for-the-design-and-construction-of-ac-offshore-substations-for-wind-power-plants.html.

[44] DNV GL. *DNV-ST-0145 Offshore Substations*. Accessed: 2025-01-05. 2021. URL: https://www.scribd.com/document/661088378/DNVGL-ST-0145-2021.

[45] ENTSO-E. *European Offshore Grid – Offshore Technology*. Accessed: 2025-01-05. 2020. URL: https://www.entsoe.eu/fileadmin/user_upload/_library/publications/entsoe/SDC/European_offshore_grid_-_Offshore_Technology_-_FINALversion.pdf.

[46] *Visualisation Platform*. URL: https://2022.entsos-tyndp-scenarios.eu/visualisation-platform (visited on 07/30/2024).

[47] *Dutch Offshore Wind Atlas*. URL: https://www.dutchoffshorewindatlas.nl (visited on 07/30/2024).

[48] Fraunhofer ISE Energy Charts. *Energy Charts: Analysis of Energy Data*. Accessed: 2025-01-05. 2025. URL: https://energy-charts.info/index.html?l=en&c=NL.

[49] ENTSO-E. *European Offshore Grid: Offshore Technology - Final Version*. Tech. rep. Accessed: January 10, 2025. European Network of Transmission System Operators for Electricity (ENTSO-E), 2011. URL: https://eepublicdownloads.entsoe.eu/clean-documents/pre2015/publications/entsoe/SDC/European_offshore_grid_-_Offshore_Technology_-_FINALversion.pdf.

Energy & Materials Transition

Westerduinweg 3
1755 LE Petten
www.tno.nl

TNO innovation for life